Marine Geology 378 (2016) 333–349

Contents lists available at ScienceDirect

Marine Geology

journal homepage: www.elsevier.com/locate/margo

A contourite depositional system along the Uruguayan continental margin: Sedimentary, oceanographic and paleoceanographic implications

F. Javier Hernández-Molina [a,*], Matías Soto [b], Alberto R. Piola [c,d], Juan Tomasini [b], Benedict Preu [e], Phil Thompson [f], Gianluca Badalini [f], Adam Creaser [a], Roberto A. Violante [c], Ethel Morales [b], Marcelo Paterlini [c], Héctor De Santa Ana [b]

[a] Department of Earth Sciences, Royal Holloway, University of London, Egham, Surrey TW20 0EX, UK
[b] ANCAP, Exploración y Producción. Paysandú s/n esq. Av. del Libertador., 11100 Montevideo, Uruguay
[c] Servicio de Hidrografía Naval (SHN), Montes de Oca 2124, Buenos Aires, C1270ABV, Argentina
[d] Universidad de Buenos Aires, and Instituto Franco-Argentino sobre Estudios de Clima y sus Impactos, CONICET, Buenos Aires, Argentina
[e] Chevron Upstream Europe, Chevron North Sea Limited, Chevron House, Aberdeen AB15 6XL, UK
[f] BG Group, Exploration (Uruguay), 100 Thames Valley Park, RG6 1PT, UK

ARTICLE INFO

Article history:
Received 10 June 2015
Received in revised form 22 September 2015
Accepted 13 October 2015
Available online 21 October 2015

Keywords:
Contourites
Sedimentary processes
Seismic stratigraphy
High amplitude reflections (HARs)
Paleoceanography
Uruguayan margin

ABSTRACT

For the first time, a multidisciplinary approach to evaluate the influence of bottom currents in the Uruguayan continental margin is presented. Bathymetric data and multichannel 2D and 3D seismic reflection profiles were used to construct a morphosedimentary map to interpret and decode sedimentary and oceanographic processes along the Uruguayan continental margin. Based on these results, an extensive contourite depositional system on the margin is described, which contains an impressive array of large erosive, depositional (drifts) and mixed (terrace) features, which have been generated primarily by the near-bottom flows associated with water masses of Antarctic and subantarctic origin. From the Eocene–Oligocene boundary up to present time, the long-term influence of water masses from higher southern latitudes, in combination with down-slope sedimentary processes have strongly controlled the overall margin morphology. Most of the features described here, were formed during the middle/late Miocene epoch due to paleoceanographic shifts that include the arrival of Antarctic Intermediate Water along the margin, which in combination with deeper Antarctic Bottom Water are fundamental in the margin evolution. In combination with Quaternary climatic and eustatic changes in sea level, fluctuations of the Brazil–Malvinas Confluence influenced subsequently glacial and interglacial stages as recognized in sedimentary features defined here. These paleoceanographic changes controlled the sedimentary stacking pattern and the locations of high amplitude reflections along the contourite terraces, which could be associated with sandy deposits. A more detailed understanding of the margin will improve interpretations of variations in the South Atlantic subtropical gyre and further constrain general climatic and ocean circulation models.

1. Introduction

Over the last decade, numerous bottom current-controlled depositional, erosional and mixed features have been recognized along continental margins and within abyssal plain regions of the world oceans (e.g., Rebesco et al., 2014). These features provide strong diagnostic evidence for both modern and ancient bottom water circulation patterns and associated sedimentary processes. Moreover, different recent works have demonstrated that bottom current circulation around continental margins is shaping their morphology and affecting their sedimentary evolution (e.g., Faugères et al., 1999; Rebesco and Camerlenghi, 2008). However, a better understanding of the processes that link the nearbottom circulation and continental slope features is needed. Other associated oceanographic processes which steer circulation of water masses (e.g., overflows, barotropic tidal currents) including intermittent processes (e.g., vertical eddies, deep sea storms, horizontal vortices, internal waves and tsunamis) are important (Shanmugam, 2006, 2012) for controlling the bottom current velocity and direction. These oceanographic phenomena remain poorly understood due to limited direct observations (Rebesco et al., 2014). Furthermore, local processes are important for contourite facies development, including the sandy contourite deposits in deep-water setting (Shanmugam, 2012; Stow et al., 2013a, 2013b), which represent an entirely different deep-water sand deposit from turbidite sands (Viana, 2008; Stow et al., 2013b). Sandy contourites are documented in some margins such as the Brazilian margin (Kowsmann and de Carvalho, 2002; Viana, 2008); the Faroe–Shetland Channel (Masson et al., 2004),

* Corresponding author.
E-mail address: javier.hernandez-molina@rhul.ac.uk (F.J. Hernández-Molina).

http://dx.doi.org/10.1016/j.margeo.2015.10.008

the Gulf of Mexico (Shanmugam, 2006, 2012) or the Gulf of Cadiz (Nelson et al., 1993; Habgood et al., 2003; Stow et al., 2013a, 2013b; Hernández-Molina et al., 2014). These deposits are mainly defined along contourite terraces (e.g., Viana, 2008) and at the exit of straits affected by overflows (e.g., Nelson et al., 1993; Hernández-Molina et al., 2014). Deep-water sandy deposits generated or affected by bottom currents are still poorly known but should be explored and evaluate, since these deposits are of great scientific and economic significance.

In the western South Atlantic large Neogene and Quaternary contourite features have been defined mainly along the Argentine (Hernández-Molina et al., 2009; Violante et al., 2010; Bozzano et al., 2011; Preu et al., 2013) and Brazilian continental margins (Viana and Faugères, 1998; Viana, 2001, 2008; Viana et al., 2002a, 2002b; Borisov et al., 2013). In summary, these studies revealed that contourite features are ubiquitous along the margin and their development is genetically linked to particular water masses and water depth range. The largest features are associated with water masses of Antarctic and subantarctic sources. Despite the strong influence the circulation exerts on present sedimentary processes in the Uruguayan margin (Franco-Fraguas et al., 2014), the lack of data has prevented the analysis of the contourite deposits in this region.

The location of the Uruguayan margin (Fig. 1) is key for the understanding of the South Atlantic bottom current processes because it is under the influence of the fluctuations of the Brazil-Malvinas Confluence (BMC), which produces large variations in the South Atlantic subtropical gyre and further constrains general climatic and global ocean circulation (Stramma and England, 1999; Piola and Matano, 2001). This work is a multidisciplinary approach with three main goals: 1) to report for the first time an extensive contourite depositional system (CDS) on the Uruguayan continental margin with a detailed morphosedimentary map; 2) to present a seismo-stratigraphic analysis for decoding both the regional stratigraphic stacking pattern and the major evolutionary stages of the CDS from the Eocene/Oligocene boundary to the present day; and 3) to discuss comprehensively the sedimentary, oceanographic and paleoceanographic implications based on the CDS distribution and evolution, with particular emphasis in determining the relationship between sandy deposits and contourite features.

2. Geological setting

The Uruguayan continental margin (Fig. 2) is a segmented, volcanic rifted margin (Soto et al., 2011). It is characterized by thick wedges of *seaward dipping reflectors* (SDRs) and more than 7 km-thick depocenters with volcano-sedimentary infill. The basin infill has been divided into four sequences (Soto et al., 2011; Morales, 2013): a) *prerift* (Paleozoic continental to marine sediments, as well as Proterozoic and older crystalline basement rocks), b) *synrift* (Late Jurassic–Neocomian volcanic rocks and continental sediments), c) *transition* (Barremian–Aptian continental to marine sediments, depending on the position within the basin) and d) *drift* (Late Cretaceous transitional to marine sediments and Cenozoic marine sediments). Besides the ill-defined Oriental del Plata Basin, two main basins of different ages are recognized offshore Uruguay (Fig. 2), with a distinct Mesozoic and Cenozoic evolution: the Punta del Este Basin to the south, and the Pelotas Basin to the north (Soto et al., 2011). They are separated in the shelf shallow waters by a basement high, the

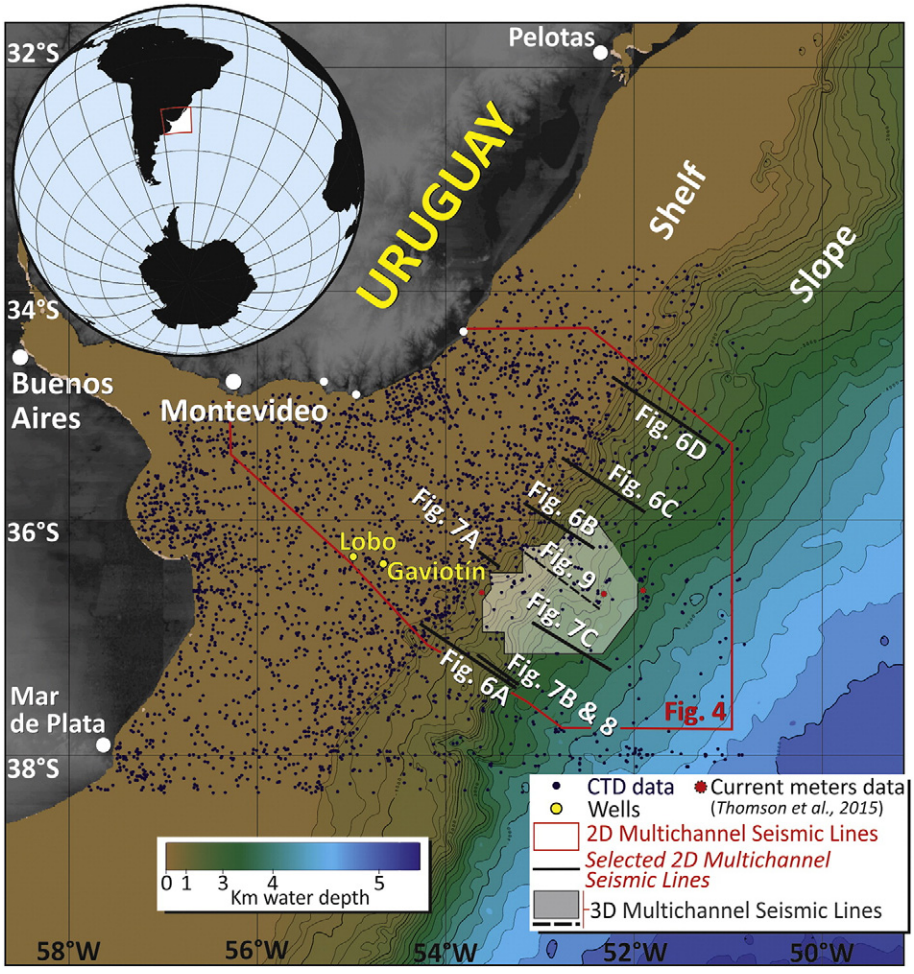

Fig. 1. Bathymetric map of the Uruguayan continental margin indicating major physiographic domains and position of dateset.

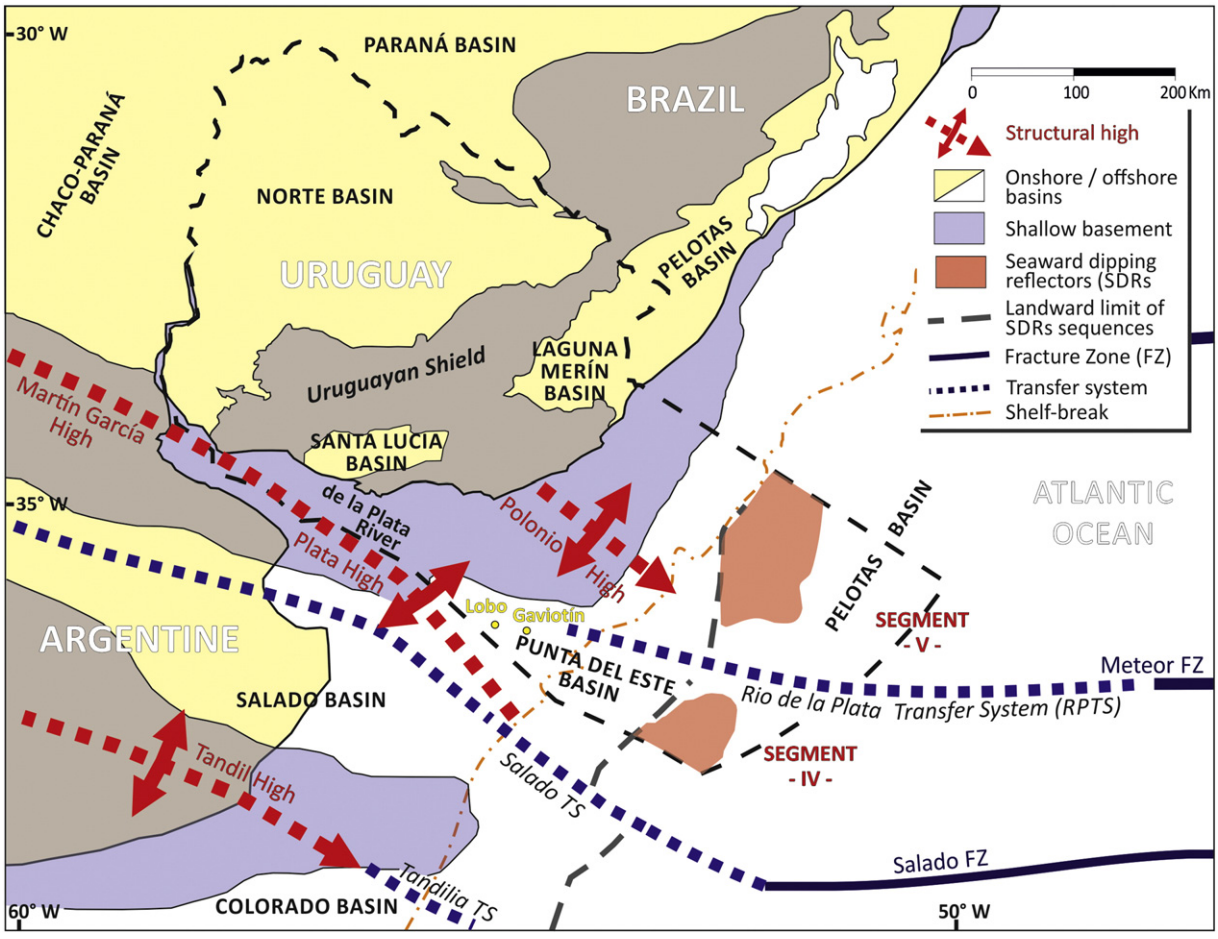

Fig. 2. Geological map of the Uruguayan continental margin depicting onshore and offshore basins and structural highs (modified from Soto et al., 2011). The landward limit of the Seaward Dipping Reflectors (SDR) sequence is based on Franke et al. (2007). The location of the Gaviotín and Lobo wells is also indicated.

so-called Polonio High (PH, Fig. 2), which played an important role as a sediment source area.

The Punta del Este Basin (Stoakes et al., 1991) is a NW–SE trending, funnel-shaped aulacogen related to the Salado Basin in northern Argentina. It displays a series of Late Jurassic–Early Cretaceous hemigrabens (with Paleozoic relicts in deeper sections) and a complex structural style, with both NW–SE and NE–SW faults controlling the hemigraben development. Following this stage of mechanic subsidence, there was an incipient thermal subsidence in the Barremian–Aptian. The Late Cretaceous sedimentation was mainly characterized by deposition of conspicuous prograding deltaic clinoforms, while the Cenozoic sedimentation was strongly controlled by Andean tectonics and uplift, as well as eustatic oscillations (Morales, 2013).

The Pelotas Basin, in turn, is a typical NE-trending passive margin that continues up to the Florianópolis Fracture Zone in Brazil. It shows poorly developed hemigrabens controlled by a simple, antithetic faulting style. Late Cretaceous sediments are scarce compared to the Punta del Este Basin (with Pelotas Basin being a probable starved basin at this period), but entering the Cenozoic large volume of sediments reached the basin. Paleogene and Neogene sediments are very thick in the southern and the northern Pelotas Basin, respectively. All these mean that from the Late Cretaceous onwards, a depocenter migration was recorded offshore Uruguay (Morales, 2013).

SDR wedges, as well as the magnetic anomalies associated to them, are dissected by the Rio de la Plata Transfer System (RPTS; Soto et al., 2011), similar to those already recorded offshore Argentina (Franke et al., 2007; Blaich et al., 2009). Distally, as proposed by Stica et al. (2014), the RPTS may extend into the Meteor Fracture Zone (Fig. 2). The RPTS (related to the southern boundary of the Polonio High) has divided the Uruguayan margin into two main sectors, each corresponding to one of the already mentioned basins. A third, central sector (heavily affected by a set of NW–SE faults) can be recognized, with distinct features such as the absence of SDRs, near mantle exhumation (resembling hyperextended margins), and the presence of a distal, restricted basin of inferred Aptian age.

3. Oceanographic framework

Ocean circulation along the western boundary of South Atlantic presents a variety of water masses of northern and southern origin that flow close to the ocean bottom in opposite directions (Fig. 3). The upper ocean circulation along the Uruguayan margin results from interactions between the southward flowing Brazil Current (BC), which includes Tropical Water (TW) and South Atlantic Central Water (SACW) components, with the northward flowing Malvinas Current (MC), with primary contributions of Antarctic Intermediate Water (AAIW) and Upper Circumpolar Deep Water (UCDW). While the BC flow is strongly baroclinic and characterized by relatively high eddy kinetic energy, the MC is a relatively stable flow with an equivalent barotropic structure (Vivier and Provost, 1999), as it is topographically steered, with its main core approximately following the 1400 m isobath (Piola et al., 2013). The encounter of the BC and the MC at around 38°S creates the Brazil–Malvinas Confluence (BMC, Fig. 3) (Gordon and Greengrove, 1986; Stramma and England, 1999; Piola and Matano, 2001). The confluence is characterized by sharp horizontal fronts in temperature and salinity and intense mesoscale variability which causes high-amplitude meandering of the mean flow and the formation of eddies which vertically extend beyond the main thermocline

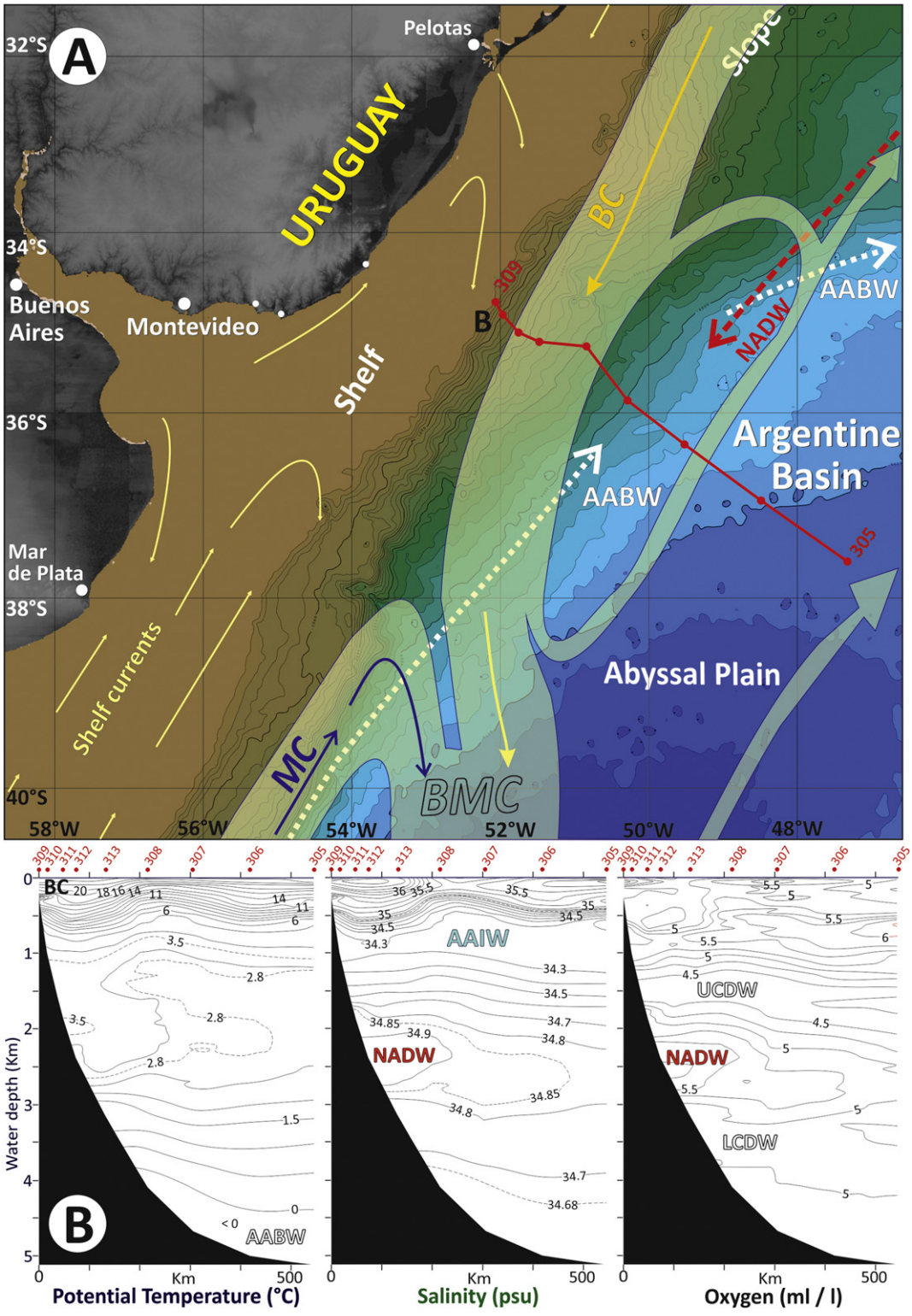

Fig. 3. A) Bathymetric map indicating schematic position of water masses and datasets. B) Hydrographic section showing lateral variations in potential temperature (°C), salinity and dissolved oxygen (ml/l). Location in A. Abbreviations: AABW = Antarctic Bottom Water; AAIW = Antarctic Intermediate Water; BC = Brazil Current; BMC = Brazil–Malvinas Confluence, LCDW = Lower Circumpolar Deep Water; MC = Malvinas Current; NADW = North Atlantic Deep Water; UCDW = Upper Circumpolar Deep Water.

(e.g. Gordon, 1989). The poleward migration of the BC generates eddies which might strongly influence the underlying water stratification (Gordon and Greengrove, 1986; Gordon, 1989).

Meridional migrations of several hundred kilometers of the separation point of the BC from the margin have been documented (e.g., Olson et al., 1988; Saraceno et al., 2004; Lumpkin and Garzoli, 2011). Satellite derived sea surface temperature and height data collected between 1993 and 2008 indicate the migration of the separation of the BC from the 1000 m isobath spans between 34.5 and 40°S (Goni et al., 2011). These studies also indicate that the BC may undergo interdecadal migrations in response to changes in the basin-wide wind stress curl (Lumpkin and Garzoli, 2011). Though direct current observations in

this region are not available the migrations of the confluence separation point must have a profound effect on the upper ocean circulation along that portion of the upper margin. Another relevant aspect of the circulation near the upper continental margin is the evidence from in-situ and satellite observations and high-resolution simulations of substantial cross-shore flow of low-salinity shelf waters with Rio de la Plata contributions along the BMC axis (Guerrero et al., 2014; Matano et al., 2014). The above described migrations of the BC separation are likely to also affect the location of the export of shelf waters as suggested by Matano et al. (2014).

The meridional extent of the subsurface water masses along the margin, and their variations is poorly understood. In an attempt to identify the regions of interaction among water masses and the ocean floor along the western margin of the Argentine Basin, Preu et al. (2013) analyzed near-bottom potential temperature, salinity and dissolved oxygen distributions from high-quality historical observations. Their analysis suggests that most of the SACW ($\theta > 8$ °C, $S > 34.8$) deviates from the margin near 36°S while northward flowing low-salinity ($S < 32.25$) AAIW appears to flow northward along the margin to ~30°S. These observations are in contrast with previous analyses which reported a sharp transition of AAIW across the BMC (e.g., Piola and Gordon, 1989). However, given the sparse observations along the boundary neither of these results is conclusive. The near-bottom properties distribution also suggests that southward flowing "recirculated" AAIW is in contact with the bottom only up to 29°S, while North Atlantic Deep Water (NADW) reaches close to 38°S (Fig. 3). Thus, the results of Preu et al. (2013) suggest that, in contrast with the near surface layer, there is no clear near-bottom transition of water masses of southern and northern origin in the narrow strip along the western boundary.

The abyssal circulation is dominated by the Antarctic Bottom Water (AABW, Fig. 3), which is partially trapped in the Argentine Basin. The containment of the AABW generates a large regional-scale cyclonic gyre (up to 2 km thick), whose influence is apparent at depths greater than 3.5 km (GEORGI, 1981; Stramma and England, 1999).

4. Methodology

The present work is based on a new regional database comprising oceanographic, bathymetric, MultiChannel 2D and 3D Seismic reflection profiles (MCS) and well data (Fig. 1). Oceanographic analysis was performed using conductivity, temperature and depth (CTD) stations integrated with acoustic analysis.

Hydrographic data from the World Ocean Database 2009 (WOD09) was used to create the joint hydrographic and seismic cross sections. Due to the lack of synoptic hydrographic sections we constructed the cross-slope sections by combining all available CTD stations and projecting water sample stations onto the seismic cross-section at distances of up to 30 km. To reduce noise related to variation in water mass distributions, the fields are smoothed to better represent the time-mean property distributions. This approach provided a dataset large enough to suppress small-localized features and seasonal events. The projection distance provided sufficient resolution for clearly identifying regional changes in the hydrographic profile. The cross-sections were created using Ocean Data View (Schlitzer, 2013). CTD data were also used for generating potential temperature-salinity diagrams. Finally, data from three current meters located offshore Uruguay recently reported by Thompson et al. (2015) at 0.5, 3 and 3.5 m over the sea floor have been considered (Fig. 1). These current meters were recorded over a consecutive 3-week period.

Bathymetric data were collected by the Uruguayan Navy while the multichannel 2D and 3D seismic data have been collected over the last decades by the Administración Nacional de Combustibles, Alcohol y Portland (ANCAP, the national oil company of Uruguay), British Gas (BG) Group, Compagnie Générale de Géophysique (CGG), Wavefield Inseis, and the *Bundesanstalt für Geowissenschaften und Rohstoffe* (BGR). 3D Pre-Stack Depth Migration (PSDM) seismic data compiled by BG Group covers approximately 13,000 km^2 in the southern Pelotas Basin (Fig. 1).

Morphosedimentary features were identified and mapped using bathymetry and seismic profiles. Conspicuous stratigraphic horizons and discontinuities were interpreted based on 2D and 3D MCS and well data, and the regional nomenclature adopted for the Argentine margin and southernmost part of the Uruguayan margin follows Ewing and Lonardi (1971), Hinz et al. (1999), Franke et al. (2007), Hernández-Molina et al. (2009), Violante et al. (2010) and Gruetzner et al. (2011). Seismic interpretation was performed using the Kingdom Suite™ (IHS) software package for the 2D seismic project and using Petrel (Schlumberger software) for the 3D seismic data set. Only two exploratory wells (Lobo and Gaviotín, Figs. 1 and 2) were drilled offshore in 1976 by Chevron in shallow waters (40–50 m) in the Punta del Este Basin, although they are not representative of the deepest part of the basin. These two wells have contributed some understanding of the stratigraphic succession (Morales, 2013). The stratigraphic horizons AR4, AR5 and TMM were correlated to these wells, following Morales (2013) criteria. Furthermore, the regional horizons H2 and H1 were assigned based on lateral correlation with the northern Argentine margin (Violante et al., 2010; Preu et al., 2012, 2013). Seismo-stratigraphic analysis of the Punta del Este Basin extends in a northward direction only to the PH, beyond which mass transport deposits (MTDs) and other prevalent, large-scale erosional surfaces obscure the interpretation of selected horizons.

The term 'contourite' refers to sediments deposited or substantially reworked by the persistent action of bottom currents (e.g., Rebesco and Camerlenghi, 2008). Contourites include a wide array of sediments affected to varying degrees by different types of currents (Rebesco et al., 2014). Thick, extensive sedimentary accumulations are referred to as contourite drifts or simply drifts. For the present work, we adopted the classification of Faugères et al. (1999) (later updated by Faugères and Stow, 2008) and use the local and regional names for drifts described by previous authors in the northern Argentine margin (e.g., Hernández-Molina et al., 2009; Violante et al., 2010; Preu et al., 2012, 2013).

5. Morphosedimentary features

Recent morphological features distribution exhibits affinities to northern and southern sectors, coinciding with the respective Punta del Este and Pelotas basins (Fig. 4). Sea floor morphology in these sectors consists of a complex assortment of large-scale downslope and along-slope features.

Downslope sedimentary processes are ubiquitous in offshore areas of the Polonio High and within the northern sector. These include MTDs that appear as slides, slumps and debrites. The Cabo Polonio Mega Slide spans more than 4000 km^2 and exemplifies large-scale features associated with downslope processes (Fig. 4). Debrites predominate in the lower slope-rise transition zone where huge deposits are exposed on the sea floor or appear buried in seismic profiles (Fig. 5). Six large submarine canyon systems (SCS) have been identified, namely from south to north: Rio de La Plata SCS; Montevideo SCS; Piriápolis SCS; José Ignacio SCS; La Paloma SCS; Cabo Polonio SCS; and Punta del Diablo SCS (Fig. 4). These canyons reach widths of up to 6 km and incision depths of up to 800 m. These systems do not connect to modern or ancient continental drainage channels, nor do they relate to paleofluvial incisions of the shelf (Fig. 4).

Extensive contourite features occur along the entire margin, even where downslope features predominate (Figs. 4, 5 and 6). We sub-divide contourite features into depositional, erosional and mixed erosive-depositional features, which are described next.

5.1. Depositional contourite features

Depositional features include contourite drifts such as the two large plastered drifts that occur on the lower slope (D1 and D2, Figs. 4 and 5). The drift D1 is located between ~1.5 and 2.5 km water depth (wd). This

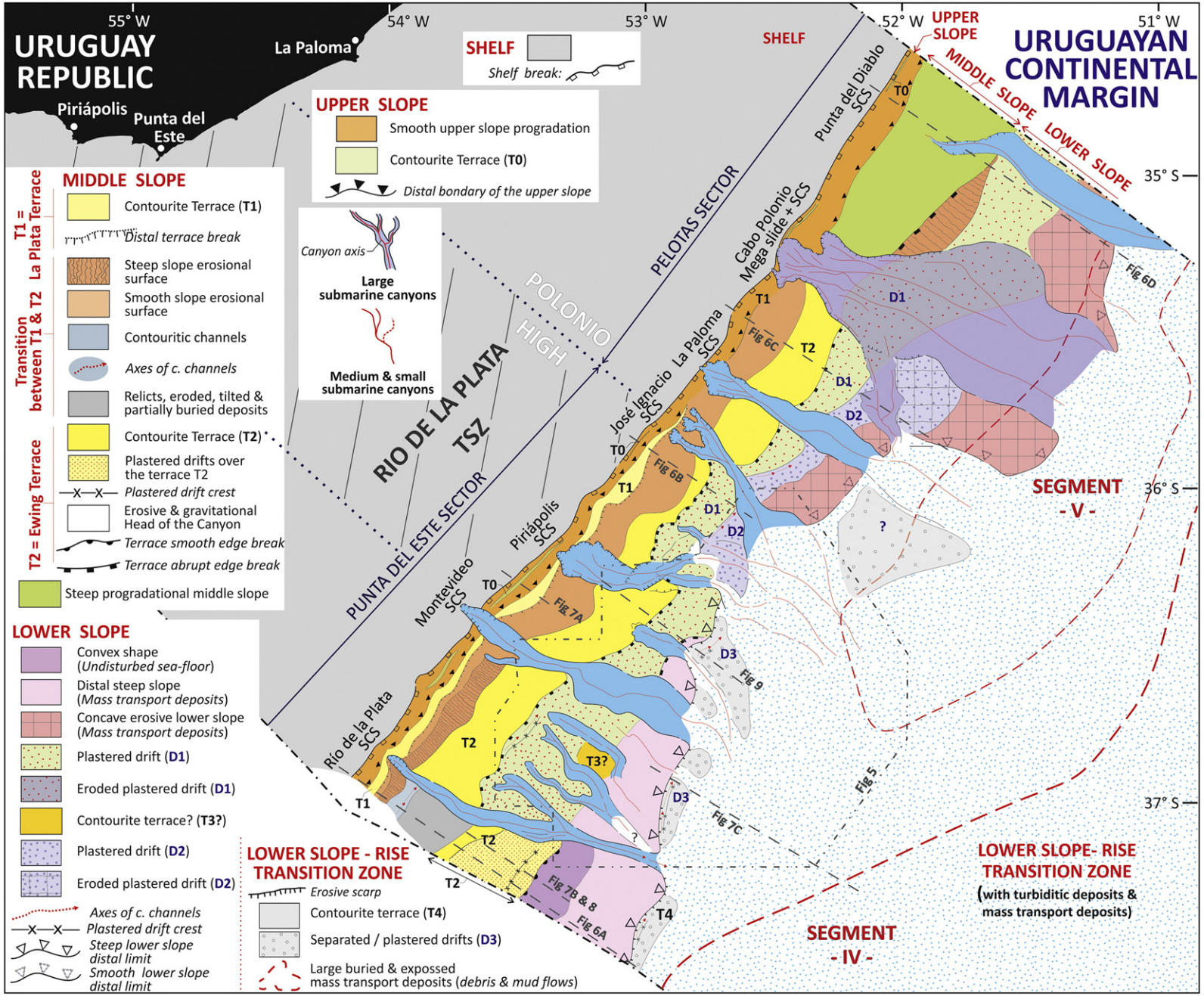

Fig. 4. Morphosedimentary map of the Uruguayan margin. This map illustrates the complex morphology of the Uruguayan continental margin as well as the interplay between down- and along-slope processes. Contourite depositional, erosional and mixed erosive-depositional features are indicated. The oceanic Segment IV and V defined by Franke et al. (2007) and Soto et al. (2011) are included. Abbreviations: SCS = Submarine Canyon Systems; TSZ = Transfer System Zone.

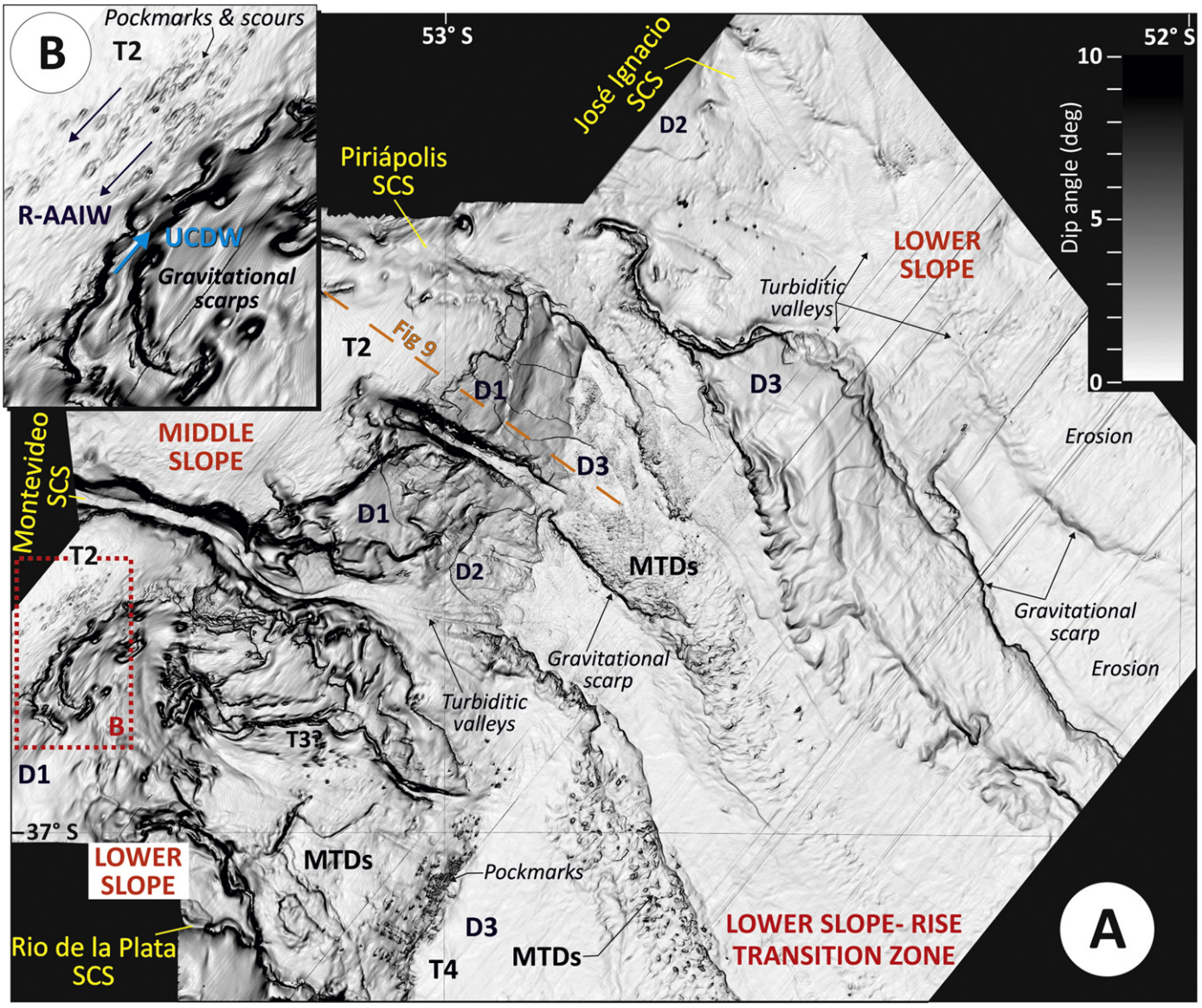

Fig. 5. A) Dip magnitude of the present-day seafloor based on 3D seismic data, showing the morphology. Location in Figs. 1 and 4. B) Detail of the highlighted area illustrating deformed pockmarks and scour/dune field related to the re-circulated (southward flowing) AAIW (R-AAIW) and Upper Circumpolar Deep Water (UCDW) circulation (courtesy of BG Group). Main submarine canyons-systems (SCS); drift deposits (D1, D2 and D3); contourite terraces (T2 and T4) and mass-transport deposits (MTDs) is indicated.

feature exhibits an aggradational to slightly progradational configuration that rises from the slope as a fairly broad (>2 km wide) and gentle mound (Fig. 6). A contourite terrace (T2) typically lies landward of and above the D1 drift. The drift D2 appears locally in the distal region of the lower slope, between ~2.5 and 3 km wd (Figs. 4 and 5). This feature has a well-defined aggradational stacking pattern and is partially eroded within its distal segment in the Pelotas sector (Fig. 6). A more isolated drift (D3) occurs along the lower slope-rise transition zone at >3.5 km wd (Fig. 4). The drift D3 exhibits smooth mounded and elongated geometry with an upslope progradational stacking pattern. This drift D3 is absent in areas affected by mass transport deposits but appears to form in association with the T4 contourite terrace at the base of the slope (BOS) in the entire margin with an adjacent moat (Figs. 4 and 5).

5.2. Erosional contourite features

Erosional features consist primarily of moats, contourite channels and erosional surfaces (Fig. 4). Large moats that reach 1.5 km in width and >100 m in depth, run parallel to isobaths and form in association with the T2 terrace and the drift D3. Local erosional scarps and surfaces occur at various depths, typically in landward positions relative to contourite terraces and moats.

5.3. Mixed features

Mixed features include the contourite terraces, which appear as subhorizontal elements (Figs. 4, 5 and 6). These are major morphologic features that developed during long-term depositional and erosive phases of the margin (Figs. 6 and 7). Proximally, these terraces have a subtle seaward tilt, increasing its angle distally. We identified a set of five more or less laterally continuous terraces at distinct depth intervals along the slope (Fig. 4), referred to as T0-T4. These develop along the outer slope (T0 and T1 at ~0.25 and ~0.5–0.6 km wd respectively), middle slope (T2 between 1.2 and 1.5 km wd), lower slope (T3 at ~2.5 km wd), and within the BOS (T4 at ~3.5 km wd).

The T0 terrace occurs discontinuously along the entire slope. T1 and T2 terraces are very well defined in the southern sector (Fig. 7), but disappear in the vicinity of the Cabo Polonio Megaslide and do not extend northward (Fig. 4). Terraces T1 and T2 represent the northern extension of the La Plata and Ewing terraces of the Argentine margin

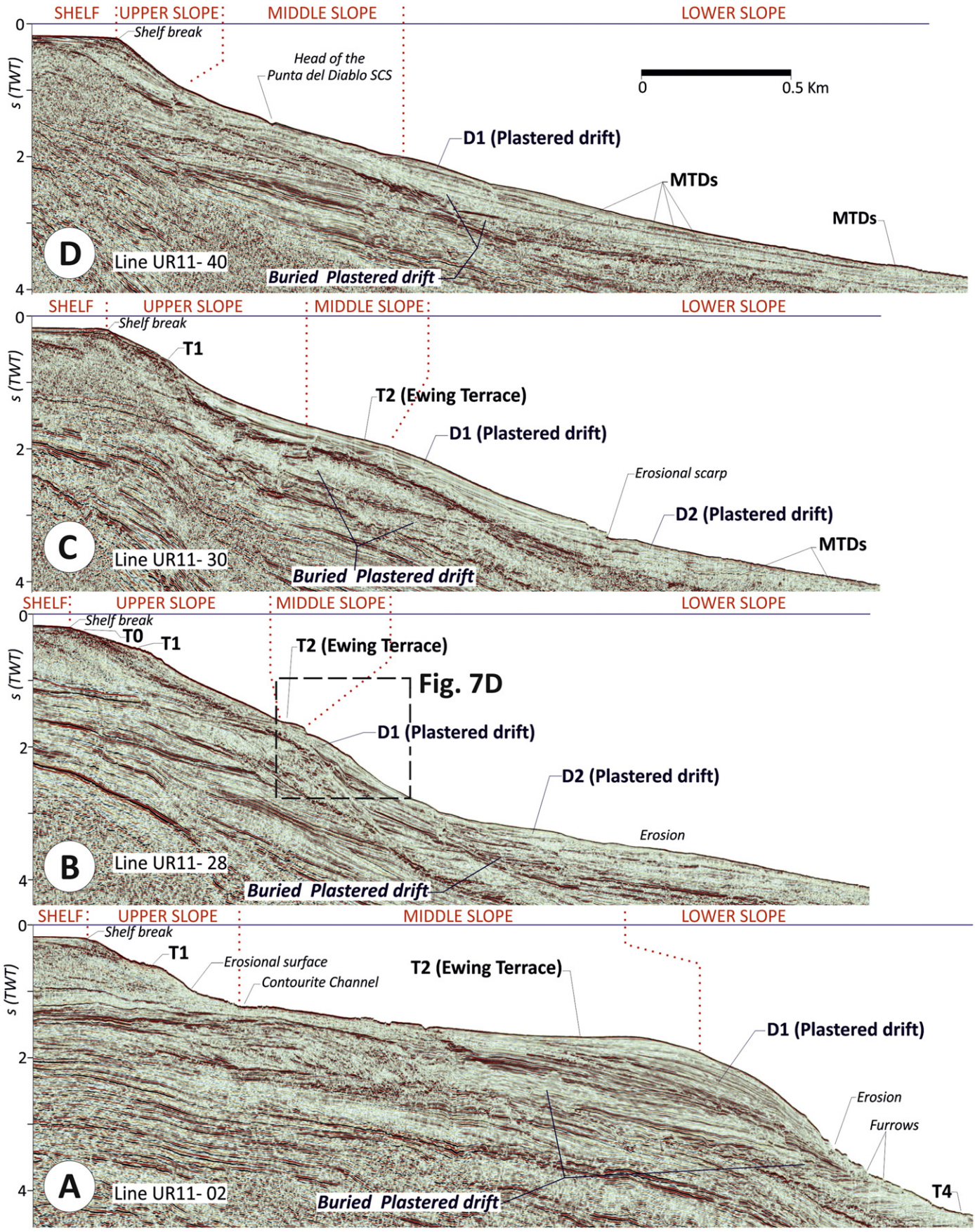

Fig. 6. Examples of four multichannel seismic reflection profiles (MCS) crossing the Uruguayan continental margin from south (A) to north (D), showing the major morphosedimentary features. Horizontal scale is the same for all the profiles. Locations in Figs. 1 and 4 (courtesy of ANCAP).

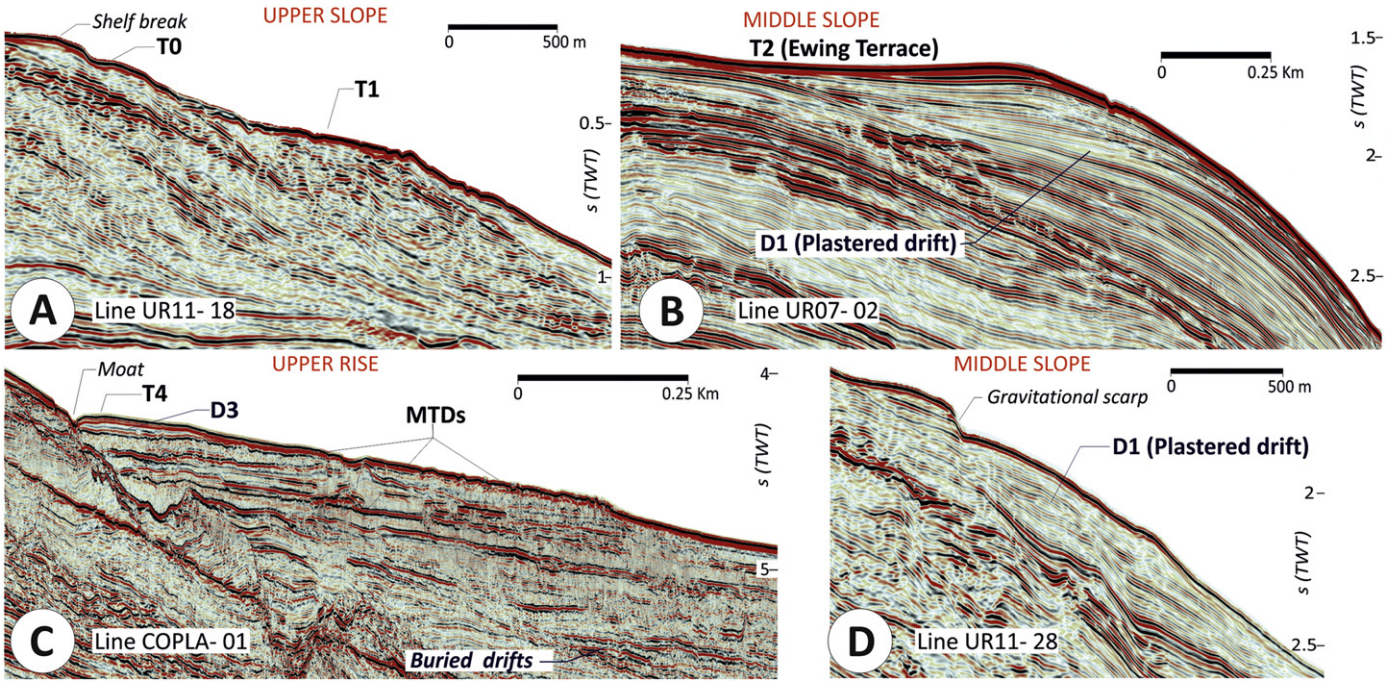

Fig. 7. Examples of some depositional and mixed contourite features on multichannel seismic reflection profiles (MCS), with profile A being the most southern and profile D the most northern. Details of contourite terraces of T0 and T1 in (A), of T2 in (B) and of T4 in (C). Examples of plastered drift D1 is illustrate both in (B) and (D) and the moat and separated drift related to D3 is showed on (C). Locations in Figs. 1 and 4 for A, B and C, and D depict details of the highlighted areas shown in Fig. 6B. Profiles A and B courtesy of ANCAP, except profile B (courtesy of Spectrum) and profile C (courtesy of COPLA).

(Hernández-Molina et al., 2009; Preu et al., 2013), respectively. The T2 terrace reaches widths of ~55 km along its southernmost edge but narrows to <20 km in the northern sector where it is affected by mass transport deposits in the Rio de la Plata Transfer System zone (Fig. 4). Locally, along the T2 terrace large horseshoe-shaped dunes have been recently identified (Thompson et al., 2015). Relative to other terraces, the T3 terrace appears only as a sporadic and poorly developed feature. In contrast, the deeper terrace, T4 exhibits good lateral continuity along the base of the slope, except where truncated by mass transport deposits (Figs. 4, 5 and 7). Since MTDs are dominant if the northern sector, the T4 terrace is more obvious in the southern sector. The T4 terrace appears to represent the extension of a terrace identified along the Argentine margin, where is it referred to as the Necochea Terrace (Preu et al., 2013). In this terrace coalesced scour field and individual large furrows parallel to the margin, which reach 400 m long and 250 m wide, has been described (Thompson et al., 2015).

6. Stratigraphic analysis

Evidence of regional bottom-current features is ubiquitous in the sedimentary record of the margin (Figs. 8 and 9), but we have focused in this work in contourite features and seismic units younger than Eocene. Five major discontinuities have been identified: AR4, AR5, TMM, H2 and H1, which delimit five main seismic units. The ages of these discontinuities are Eocene/Oligocene boundary for AR4; Middle Miocene (~16 Ma) for AR5; top of the middle Miocene for TMM (~11.6 Ma); top of the Late Miocene for H2 and Late Pliocene for H1, based on regional stratigraphic criteria from Violante et al. (2010), Preu et al. (2012, 2013) and Morales (2013).

AR4 appears as an erosional surface, and forms the base of a huge buried plastered drift that extends into the middle Miocene part of the section (Figs. 8 and 9). This erosional surface occurs along the entire margin and onlaps upslope over previous margin irregularities. The Eocene and Oligocene units tilted seaward and the middle Miocene and Pliocene units have differential subsidence, which record tectonic events occurring along the margin in these periods (Figs. 8 and 9).

A prominent change in the sedimentary stacking pattern occurs during the middle Miocene, between AR5 and TMM, when a more aggradational unit develops in tandem with development of the T2 terrace. The sedimentary stacking pattern also shows a later regional shift marking the inception of present-day slope contourite features including the plastered drifts (D1 and D2). The D1 drift evolved above the TMM during the late Miocene as a progradational wedge confined to the upper part of the lower slope (Figs. 8 and 9). The Miocene–Pliocene boundary (H2) also represents a significant change in depositional processes wherein aggradational contourite features begin their development. The H1 boundary appears as a regional stratigraphic surface during the Late Pliocene associated with a change in reflection-stacking pattern in the overlying deposits, which progrades in a landward direction.

High amplitude reflections (HARs) are frequent within submarine canyons and along the contourite terraces. They have been identified in the Oligocene, Middle Miocene, Late Miocene, Pliocene and Quaternary sedimentary record. On the contourite terraces, the HARs are seen on top of most of the plastered drifts along the slope, become weaker seaward and disappear. Probably, the best example is the Ewing terrace (T2) and associated D1 drift where these HARs are ubiquitous (Figs. 8 and 9).

7. Hydrographic cross sections

To analyze the possible relationship between the water mass structure and sedimentary features on the continental margin we present three cross-slope hydrographic sections based on all available high-quality bottle and CTD stations projected onto the seismic profiles off Punta del Este (UR11-02) and Pelotas (UR11-30 and UR11-40) (Fig. 10). Combining these sections with potential temperature–salinity diagrams prepared with the same data set (Fig. 11) has allowed us to identify the main water masses in each physiographic domain and

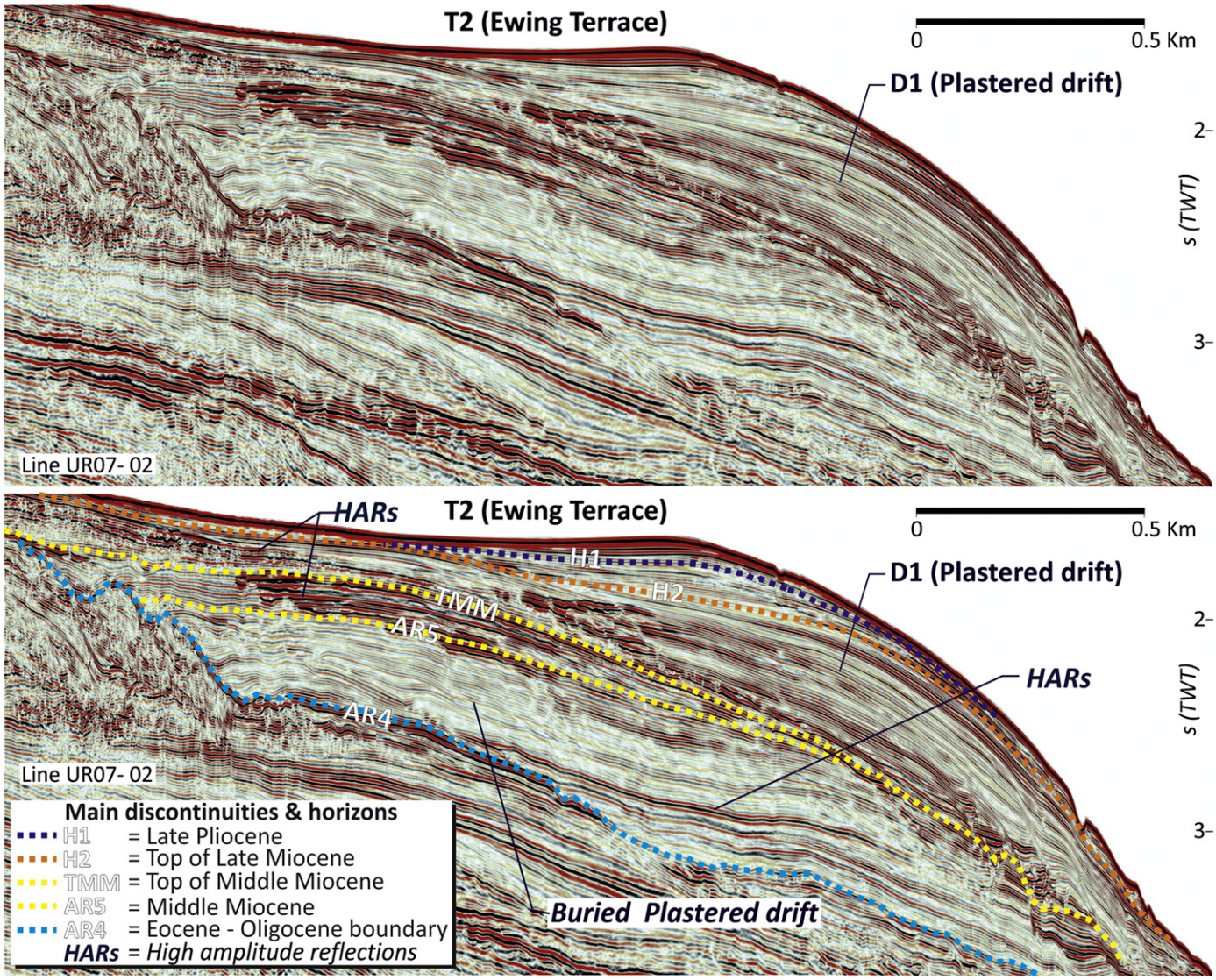

Fig. 8. Example of a MCS reflection profiles showing T2, D1, and the main stratigraphic horizons and discontinuities. Location in Figs. 1 and 4. Some high amplitude reflections (HARs) patterns of the contourite terrace are shown, which are indicative of sandy deposits; Stratigraphic horizons and discontinuities are shown in (B), with assignments for the Eocene–Oligocene boundary (AR4); early middle Miocene (AR5); top of middle Miocene (TMM); end of Late Miocene (H2) and the end of the Late Pliocene (H1).

their lateral changes along the Uruguayan continental margin. Selected neutral density profiles in this region are (Fig. 11D): 26.7 kg/m^3 for the SACW–AAIW transition; 27.5 kg/m^3 for the AAIW–UCDW; 27.87 kg/m^3 for the UCDW–NADW and 28.07 kg/m^3 for the NADW–Lower Circumpolar Deep Water (LCDW). Identification of present water masses and their correlation with the sea floor morphology is important to understand the longer-term oceanographic and sedimentary processes and its products. The present oceanic circulation offshore Uruguay is highly complex, with a number of water masses active at various depths, which are briefly described below.

7.1. Section UR11-02 (from 36.5°S to 37.5°S)

This hydrographic section is located in the southern part of the margin (Fig. 10A), and intersects the 1000 m isobath near 37°S. Due to its proximity to the BMC the upper layers along this section are somewhat noisier due to mesoscale (Goni et al., 2011) and seasonal variability (Saraceno et al., 2004). The section presents TW and SACW in the upper layers and about 50 km east of the shelf break (Fig. 10A). Relatively cold, low salinity waters, representing mixtures of MC and shelf waters are observed further inshore. Regardless of the substantial seasonal variations associated with the migration of the confluence and with the export of low salinity shelf waters (e.g., Guerrero et al., 2014) the separation between TW and SACW from the shelf break by several tenths of km is observed in both summer and winter (not shown). Thus, the data indicate there is no interaction of TW or SACW with the ocean bottom at this latitude and that the upper portions of the margin are under the influence of MC and shelf waters. At depths between 300 and ~800 m and within 50 km from the shelf break the near bottom layer is occupied by relatively fresh (S < 34.2) and high-dissolved oxygen (>6 ml/l) waters, which are indicative of the relatively new, northward flowing, variety of AAIW, which interacts with the seafloor in the upper and middle slope (Fig. 10A). Near bottom properties over the wide T2 terrace present mixtures between AAIW and UCDW. A station located close to the offshore termination of T2, presents a low salinity minimum (34.19) at 744 m depth and the near bottom salinity increases to 34.55, which lies close to the neutral density core of UCDW. The O_2 section does not show this feature due to the lack of O_2 data in

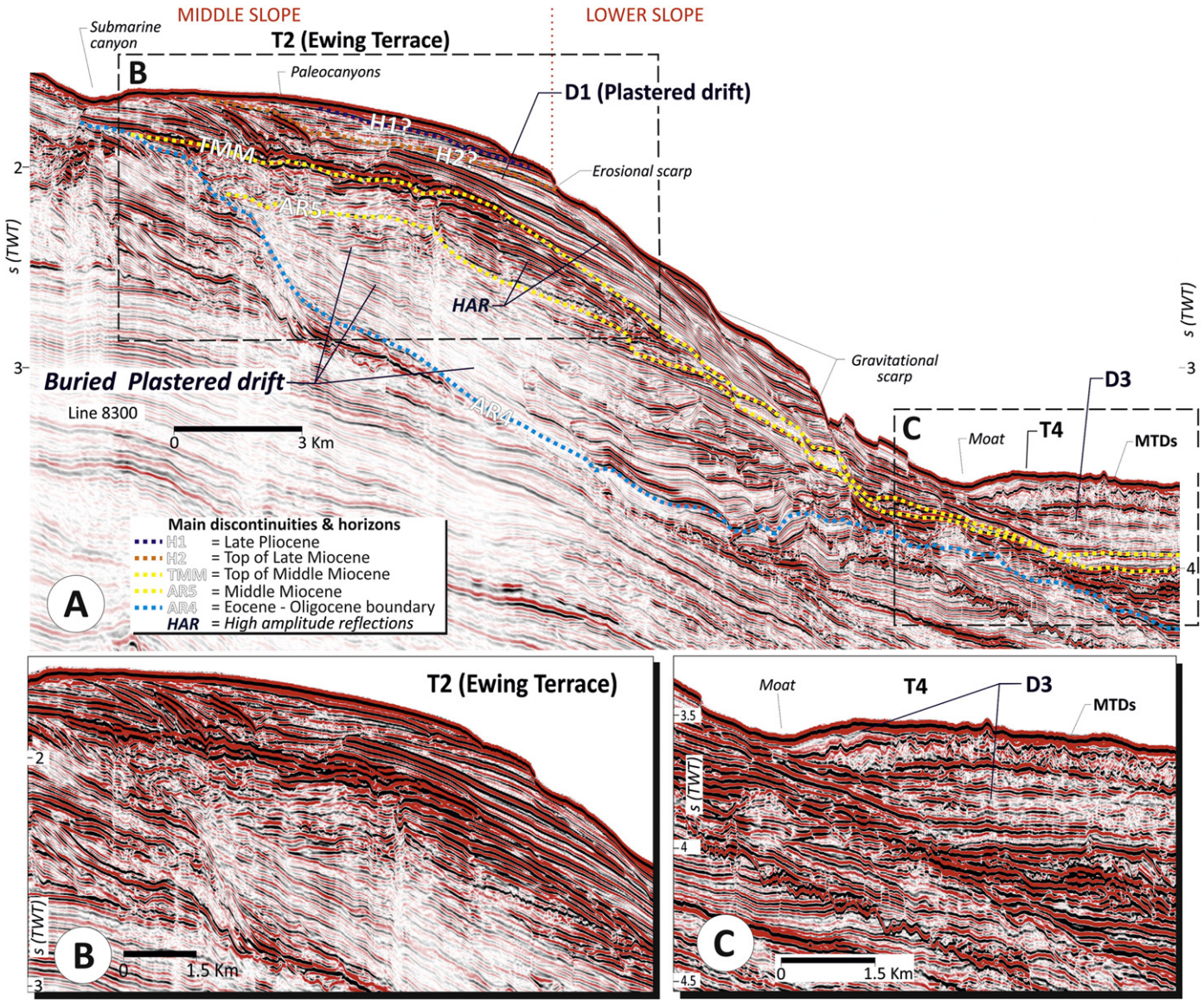

Fig. 9. MCS seismic profile (3D coverage, courtesy of BG Group) of the Punta del Este sector (location given in Figs. 1 and 4) showing contourite terraces (T2 and T4), plastered drift D1 and drift D3. At this location, Drift D2 is strongly influenced by gravitational processes in the lower slope. Stratigraphic horizons and discontinuities are shown, with assignments for the Eocene–Oligocene boundary (AR4); early middle Miocene (AR5); top of middle Miocene (TMM); end of Late Miocene (H2) and the end of the Late Pliocene (H1). Stratigraphic positions of horizons H2 and H1 are tentative due to complex regional correlation framework for this part of the margin. B) Inset depicts high amplitude reflections (HARs) patterns of contourite terrace T2, indicative of possible sandy deposits; C) Inset illustrating the drift D3 and the terrace T4, as well as the common interaction between contourites and mass transport deposits at the transition between the lower slope and upper rise.

this particular station. Below, the NADW flows southward along the margin, but its core is detached from the sea-floor (Figs. 10A and 11A). The LCDW is identified flowing north below the NADW.

The somewhat noisier distributions along this section compared with the two locations farther north is attributed to the influence of the BMC. For instance a station with low salinity (34.17) and high O2 (6.19 ml/l) AAIW at 710 depth located around bottom depth 3192 m (Fig. 10A) is surrounded by recirculated (higher salinity) AAIW. In the lower slope, the NADW (34.84, 5.01 ml/l) appears to interact with the bottom near 2000 m depth. Further offshore, at ~2600 m depth, a fresher variety of NADW (S ~ 34.78) is observed, suggesting this layer has already mixed with the fresher deep waters of southern origin. Finally, further offshore, where the bottom depth is 2870 m, the NADW core (S ~ 34.81) is about 2400 m deep, and the layer below is colder and fresher (34.77 at 2835 m), suggesting mixtures with LCDW.

7.2. Section UR11-30 (from 35.5°S to 36°S)

Along this hydrographic section the southward flowing BC is identified on the upper slope, including TW and SACW along the shelf and upper slope (Figs. 10B and 11B). Most of the AAIW layer at this section is relatively salty and lower in dissolved oxygen suggesting it has recirculated from farther north, where it has become saltier by vertical mixing on its path along the subtropical gyre. This is in contrast with the observation of low salinities (34.15) and high O_2 (6.72 ml/l) water at 610 m, where the seafloor is 705 m, indicating some "pure" AAIW flows in a narrow band along the middle slope (Figs. 10B and 11B). Similarly fresh and oxygenated AAIW is also observed further offshore, within cores of cold eddies (Fig. 10B). However, as the eddies are located away from the margin there is no interaction between AAIW and the ocean bottom.

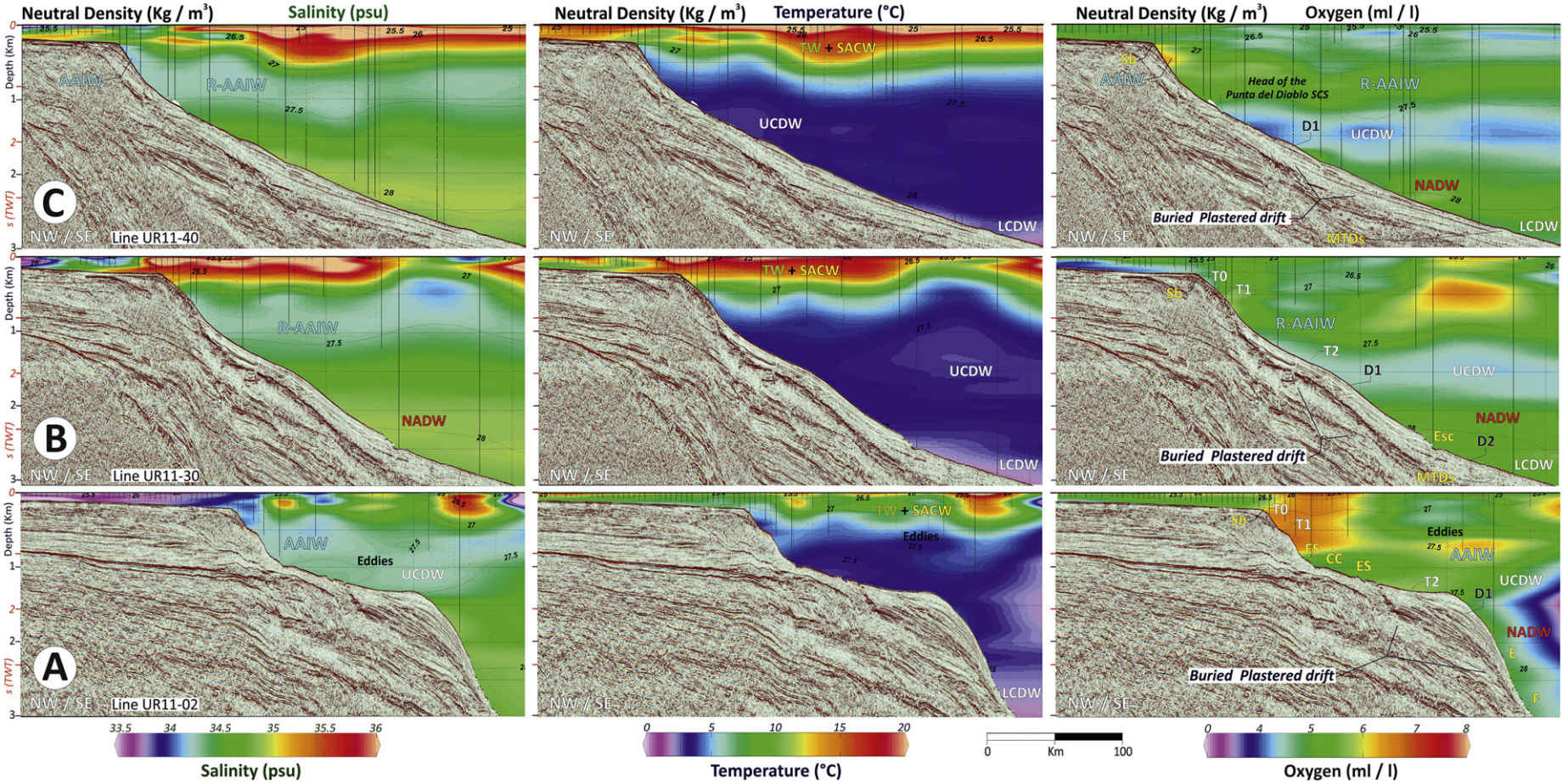

Fig. 10. Seismic and hydrographic vertical sections from the Uruguayan continental margin. The water column color ranges indicate salinity, temperature (°C) and oxygen content in ml/l. A) Seismic lines UR11-02; B) UR11-30; and C) UR11-40. These profiles are located in both Figs. 1 and 4. Water–mass interpretations and major contourite features are indicated on the sections. Section in A is in proximity to the Brazil/Malvinas Confluence (BMC) and therefore includes a greater degree of noise related to local eddy formation. *Abbreviations for water masses*: AABW = Antarctic Bottom Water, AAIW = Antarctic Intermediate Water, BMC = Brazil–Malvinas Confluence, LCDW = Lower Circumpolar Deep Water, NADW = North Atlantic Deep Water, UCDW = Upper Circumpolar Deep Water, R-AAIW = Re-circulated Antarctic Intermediate Water, SACW = South Atlantic Central Water, TW = Tropical Water. *Legend for morphosedimentary features*: CC = Contourite Channel, E = erosion, ES = erosional surface, Esc = Erosional scarp, F = Furrows, MTDs = Mass Transport Deposits, Sb = Shelf break. Contourite Terraces: T0, T1 (La Plata Terrace), T2 (Ewing Terrace), T3 and T4. Contourite Drifts: D1, D2 and D3.

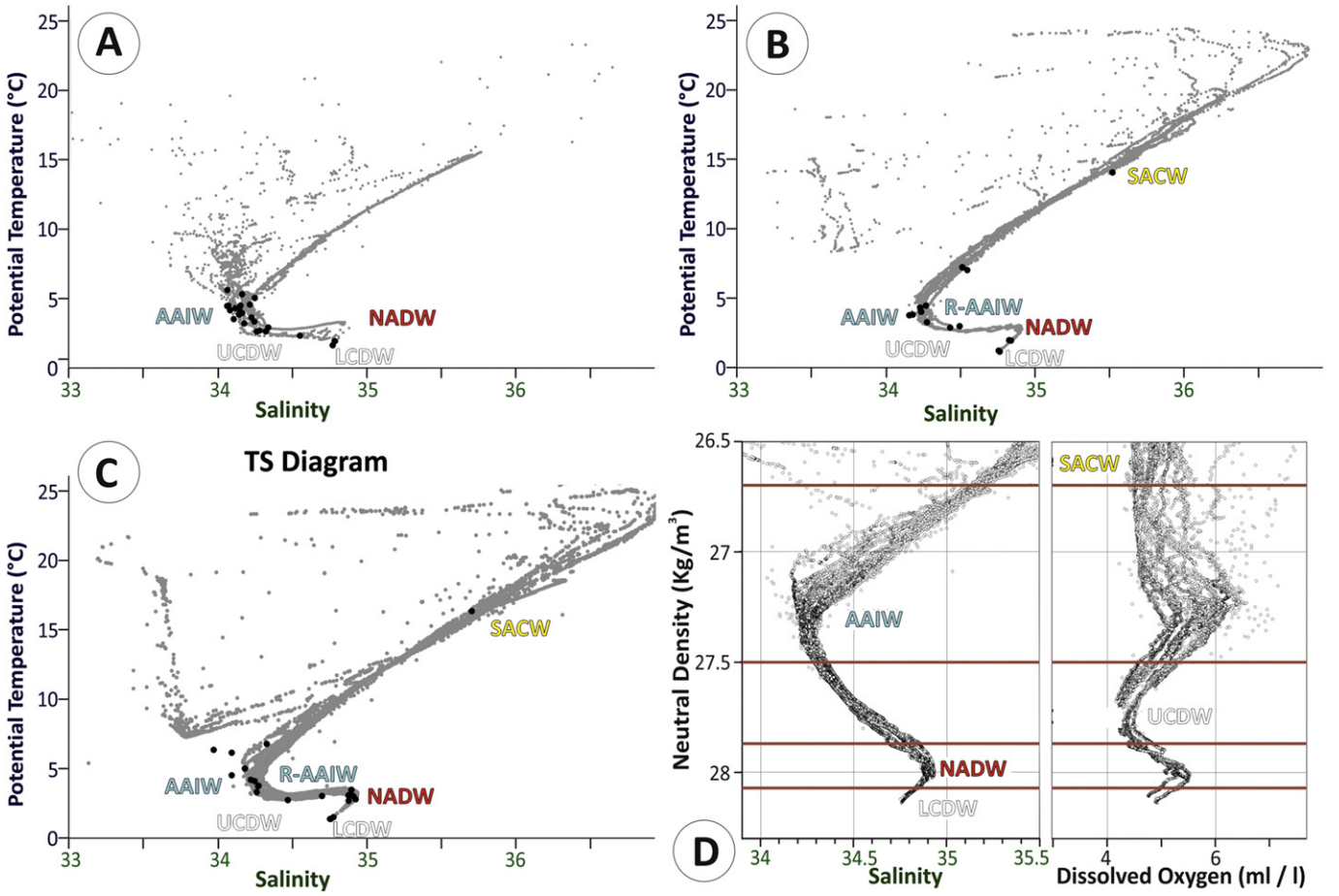

Fig. 11. Temperature/salinity (TS) diagrams for sections A, B and C of Fig. 10. Data from features at depths of less than 300 m were excluded for the sake of clarifying features not related to continental slope processes. The gray dots represent lower water column data, which display the expected water mass structure. The black dots indicate samples within 100 m above the seabed. D) Panel plot with neutral densities profiles of S and O_2 along the Uruguayan continental margin for data collected on the same seismic and hydrographic vertical sections of Fig. 10. The neutral density transitions are plotted by brown lines. Neutral densities: 26.7 kg/m^3 for the South Atlantic Central Water (SACW)–Antarctic Intermediate Water (AAIW); 27.5 kg/m^3 for the AAIW-Upper Circumpolar Deep Water (UCDW); 27.87 kg/m^3 for the UCDW- North Atlantic Deep Water (NADW) and 28.07 kg/m^3 for the NADW- Upper Circumpolar Deep Water (LCDW).

The O_2 data shows that the proximal parts of the lower slope are affected by the UCDW, which is characterized by a relative O_2-minimum near 1500 m. The lowest oxygen in the UCDW ($O_2 < 4.5$ ml/l), and therefore its less-mixed variety, is only observed in the offshore stations, and is not in contact with the ocean bottom. Thus, in section UR11-30 only recirculated, and possibly southward flowing, UCDW interacts with the bottom along the middle margin. In the lower slope the core of NADW (2.82 °C, 34.9 and 5.46 ml/l) appears to be attached to the sea floor at around 2350 m. Further deep down the slope a core of cold (1.42 °C), low salinity (34.76) and low O_2 (4.92 ml/l) bottom layer can be observed at ~2980 m depth and is a clear indication of LCDW (Figs. 10B and 11B).

7.3. Section UR11-40 (from 34.5°S to 35.5°S)

The hydrographic section in the northern sector of the margin presents the southward flowing BC, which includes TW and SACW along the shelf and upper slope (Fig. 10C). In the upper and middle slope, at a depth of 480 m a low salinity (~34.18) and high O_2 (>6 ml/l) near-bottom layer, associated with AAIW can be observed (Fig. 10C). The low-salinity and high oxygen concentration is characteristic of relatively new, northward flowing AAIW. These observations indicate that the fresh variety of AAIW penetrates northward along the upper margin to 34.5°S, beyond the location of the Brazil/Malvinas Confluence, as suggested by Preu et al. (2013). Further offshore saltier (>34.2) and lower O_2 (<6 ml/l) waters at the salinity minimum are observed. This recirculated variety of AAIW lies at mid depth and is not in contact with the ocean bottom.

A cold (2.8 °C), low O_2 bottom layer (4.22 ml/l), can be observed at 1317 m. This indicates UCDW interacting with the seafloor in the lower slope (Fig. 10C). Further down the slope about 75 km east of the shelf break and at depth of 2330 m we identify the high salinity core (S > 34.9) and high O_2 characteristic of NADW (Figs. 10C and 11C). A cold ($\theta < 1.6$ °C), low-oxygen ($O_2 = 4.9$ ml/l) bottom layer near the offshore end of the section indicates LCDW interacting with the sea bottom at the base of the slope (Figs. 10C and 11C).

8. Discussion

The regional morphosedimentary map (Fig. 4) illustrates the complex morphology of the Uruguayan continental margin as well as the interplay between down- and along-slope sedimentary processes. The headlands of submarine canyon systems reach both the shelf break and terraces T1 and T2. As such, the canyons incise into the Pliocene and Quaternary sedimentary sections but are also affected by mass transport deposits (MTDs) on the lower slope and rise (Figs. 4 and 5).

Large-scale MTDs are very common along the Uruguayan continental margin, especially on the lower slope and the transition between the slope and the continental rise. Widespread mass transport deposits occur primarily in the Rio de la Plata Transfer System and Pelotas sector indicating a greater degree of margin instability in those regions. Their occurrence on the slope has been documented previously in

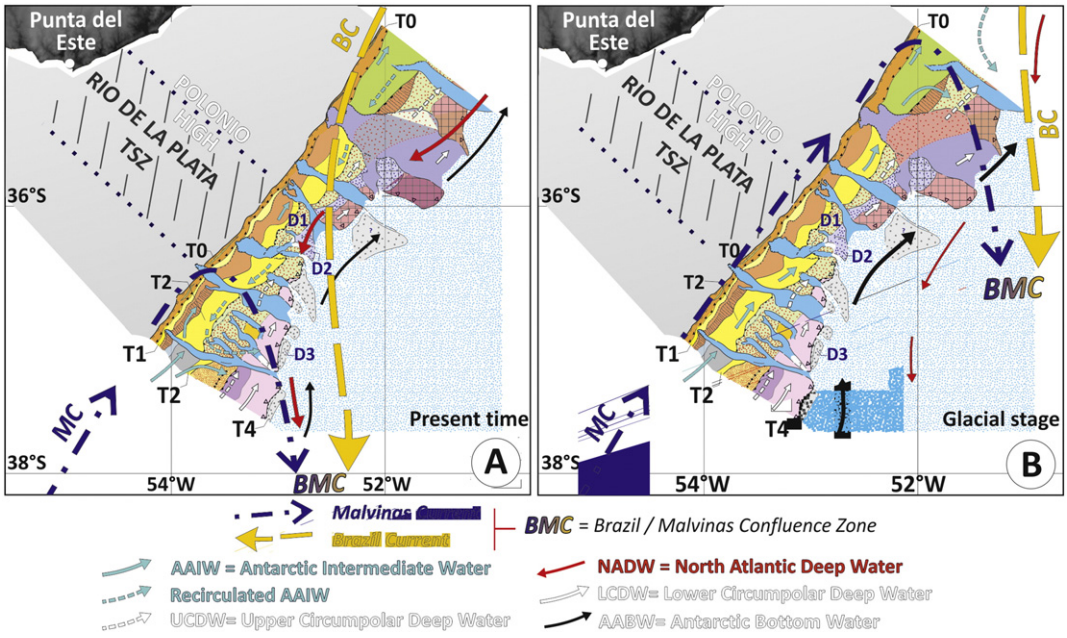

Fig. 12. Schematic drawing of the water mass circulation in plan view for A) present time based on major contourites features distribution presented in this work and available oceanographic data and B) hypothetical reconstruction for a more northern position of the Brazil/Malvinas Confluence Zone (e.g., glacial stages). Fluctuations of the Brazil–Malvinas Confluence influenced subsequently glacial and interglacial stages and have controlled the margin morphology features, such as the contourite terraces formation and their lateral continuation. These fluctuations should have been related to variations in the wind pattern over the South Atlantic and further constrain general climatic and more regional/global ocean circulation models. A simplified version of the morphosedimentary map in the background is included. See Fig. 4 for the map captions.

bathymetry data (Preu et al., 2013), in sediment cores (Krastel et al., 2011) and seismic data (Henkel et al., 2011; Tomasini et al., 2011; Preu et al., 2013). Controlling factors in their generation could be a combination of processes: a) gas hydrates occurrence and fluid migration (Tomasini et al., 2011; Gray, 2014); b) earthquakes (Krastel et al., 2011); c) recent Incaic and Quechua tectonic phases in the Andean Range (Contreras et al., 2010), which stimulate instability events in the margin; and d) unconsolidated contourite drift sediments susceptible for triggering slides (Rebesco and Camerlenghi, 2008).

8.1. Contourite features: Decoding the bottom-current processes

Contourite depositional and erosional features form over geological time scales due to the interaction between near-bottom currents of regional water masses and their interfaces along the margin (Hernández-Molina et al., 2009). The contourite depositional, erosional and mixed features described here are locally modified by submarine canyons and gravitational processes.

Contourite terraces in the Uruguayan margin are formed in association with water mass interfaces. The T0 terrace coincides with the upper depth range of the SACW. The La Plata Terrace (T1) matches the depth ranges of the BC and AAIW while the Ewing Terrace (T2) coincides with the AAIW–UCDW interface at a water depth range of 1.2 to 1.5 km. The T3 terrace occurs very locally at around 2.5 km wd in the southern sector, but does not coincide with the present depth range of a specific water mass in the immediate study area. Nevertheless, the T3 terrace does coincide with the depth of the UCDW–LCDW interface in the vicinity of the Argentine margin (Hernández-Molina et al., 2009). The T4 terrace is presently under the influence of the LCDW but coincides with the proposed depth range of the LCDW–AABW interface during past glacial eras (Preu et al., 2013). This indicates that this terrace was mostly formed during glacial periods.

Contourite drifts D1 and D3 are extensive features (on the order of 10^2 km) that exhibit pronounced lateral continuity along the entire margin. The D2 drift however is more spatially limited. The D1 drift located between ~1.5 and 2.5 km wd, includes muddy, silty or sandy sedimentary facies (Krastel et al., 2011). Along the Argentine margin these drift and facies have been attributed to northward circulation of the UCDW (Preu et al., 2013). We similarly interpret their presence along the lower slope of the Uruguayan margin in association with sea-floor features (Fig. 12) as additional evidence of northward UCDW circulation. However, in the present-day part of the D1 drift falls within a depth range currently occupied by the weak southward flow of the NADW (Figs. 10 and 12A). The D2 drift is located deeper than the D1 drift (~2.5 and 3 km), and may arise from the present-day influence of both the NADW and LCDW (Figs. 10 and 12A). If the BMC was located further north and the NADW was weaker and less extensive during glacial stages (Knutz, 2008), both D1 and D2 drifts could correlate entirely with the respective depth ranges of UCDW and LCDW. During these stages the T3 terrace forms along the interface between these two water masses (Fig. 12B).

Although the regional distribution of features at the base of the slope is indicative of a dominant northwest flow of the LCDW (e.g., furrows, reworked pockmarks, scours; Fig. 5) present current meter data (Thompson et al., 2015, Fig. 1) at the base of slope (3 km wd) and its transition with the continental rise (3.5 km wd) is highly variable. At these locations the bottom current velocity ranges from 0 to 35 cm s^{-1}, and appears to be changing from ENE to ESE. Over a 7 day period the near-bottom currents showed dramatic changes (at time scales shorter than 24 h) in the current orientation by a 180° reversal accompanied by a slight change in velocity. This change could be due to interaction of local eddies and deep tidal influences with local bottom physiography. Further bottom current data are necessary to fully understand these variations in seasonal scales.

The D3 drift is a consistent, mounded, elongated and separated drift, which evolved locally to a plastered drift, located >3.5 km wd, with a landward moat in certain localities. The drift D3 falls under the influence of the northward circulation of the AABW, a current that widens and intensifies during glacial stages (Preu et al., 2013).

8.2. Lateral migration of the Brazil–Malvinas Confluence Zone

The La Plata (T1) and Ewing (T2) terraces are currently influenced by the upper and lower boundaries of the AAIW, which, in a time

averaged sense, circulates northward along the Argentine margin (Hernández-Molina et al., 2009; Preu et al., 2013). These two terraces run continuously from the Argentine to the Uruguayan middle slope up to the Cabo Polonio megaslide, where they vanish. The features offer morphological evidence of the point at which the AAIW diverges at geological scale from the slope to circulate eastward and merges with the South Atlantic subtropical gyre (Fig. 12A). However, at present, the Ewing Terrace (T2) on the Uruguayan slope is mainly under the influence of the re-circulated (southward flowing) AAIW (beneath the BC). Current meter data (Thompson et al., 2015, Fig. 1) determine that along the Ewing Terrace at 0.5 km wd the mean bottom current orientation is towards the WSW, with a mean bottom current velocity of 10 ms^{-1} (maximum of >20 ms^{-1}), being clearly affected by tidal variations. This dominant flow pattern is particularly evident from the extensive reworked pockmarks and scour/dune features found on the terrace surfaces (Fig. 5). This apparent discrepancy in flow direction may be due to the northward migration of the Brazil/Malvinas Confluence Zone during cold (i.e., glacial; Fig. 12B) periods and to its present position during warmer (i.e., interglacial; Fig. 12A) periods. Our interpretations suggest that the progressive migration of the BMC and its near-bottom current reversals affect most of the Uruguayan margin. These results are fundamental for the subsequent sedimentary and paleoceanographic reconstructions since the lateral and vertical variation of the BMC due to the Quaternary climatic and eustatic changes are associated with the location and intensity of the subtropical gyre in the entire south Atlantic (Stramma and England, 1999).

8.3. Evolutionary stages

Regional stratigraphic analysis revealed remarkable changes in the post-Eocene sedimentary stacking pattern and four subsequent evolutionary stages (Figs. 8 and 9). Stage I represents the formation of large, thick sedimentary drifts along the entire slope overlying the Eocene–Oligocene boundary and continuing into early Miocene parts of the section. During this phase, the opening of the Drake Passage (Maldonado et al., 2014) permitted circulation of Antarctic-sourced water masses along the margin (Hernández-Molina et al., 2009). A high sediment supply accompanied this incursion (Contreras et al., 2010).

An aggradational Stage II affected the middle and lower slope, initiating the formation of most of the present-day slope contourite features. Among these features, the T2 (Ewing) terrace developed during the middle Miocene (Figs. 8 and 9), thus marking the beginning of the AAIW circulation. The onset of this water mass may be a result of changes that took place during the Middle Miocene, when Antarctic ice sheets were re-established and sea level was lowered (Zachos et al., 2001), causing a major, global reorganization in deep-sea sedimentation and hiatus distribution patterns, and limiting the production of AABW, which became further restricted to depths below ~5500 m (Sykes et al., 1998).

Later, during Stage III a remarkable change in the sedimentary stacking pattern occurred, indicating a major regional paleoceanographic shift which initiated the development of many of the slope contourite features described here, including the plastered drift D1. This paleoceanographic event coincides with similar changes along the entire Argentine margin (Hernández-Molina et al., 2009). During the last Stage IV, from the late Pliocene through the Quaternary the present-day seafloor morphology developed.

These developmental stages and paleoceanographic events coincide with climatic and eustatic sea-level changes (Miller et al., 2011), variation in global circulation (Knutz, 2008) and Incaic and Quechua tectonic episodes of the Andean orogeny (Contreras et al., 2010). Tectonic events have exerted both long- and short-term influence that invite further investigation regarding their relationship to sediment supply, sedimentary stacking pattern, water masses circulation, fluid migration, mass transport deposits and margin instability. Tectonic events of the Andean orogeny, in tandem with similar events along the SE Brazilian margin (Contreras et al., 2010), have influenced the Uruguayan margin (Rossello et al., 2009). In light of these factors, the tilting and subsidence intervals of the slope determined between AR4 and TMM may coincide with significant sediment transport events around the Eocene–Oligocene boundary and the Miocene. Sedimentation may have been triggered by subsidence intervals during the Incaic and Quechua episodes of the Andean orogeny (Benavides-Cáceres, 1999; Contreras et al., 2010). Compressive events during the Quechua phase, in turn, co-occur with major shifts in the sedimentary stacking pattern along the margin. The younger subsidence interval identified between H2 and H1 coincides temporally with the final active compressive phase of the Andean orogeny (Yrigoyen, 1979). These tectonic events could be responsible for differential subsidence observed at different points along the margin, and may have triggered the formation of mass transport deposits.

8.4. High amplitude reflections

High amplitude reflections (HARs) are frequent within submarine canyons and along the contourite terraces (Figs. 8 and 9) across the Uruguayan margin. Similar seismic facies were described in the Pliocene sedimentary record of the Gulf of Mexico (Shanmugam et al., 1993); the Eocene deposits in the Campos Basin, Brazil (Mutti et al., 1980; Viana and Rebesco, 2007) and around the Iberian continental margin (Hernández-Molina et al., 2011, 2014). In these examples the seismic facies correspond with contourite deposits mainly composed by medium- to fine-grained sand with common bedforms, such as megaripples and sand waves (Nelson et al., 1993; Viana et al., 1998, 2002b; Stoker et al., 1998; Masson et al., 2004; Mutti and Carminatti, 2012; Hernández-Molina et al., 2014). IODP expedition 339 drilled similar seismic facies along the contourite depositional system of the Gulf of Cadiz and reported clean, well-sorted contourite sands up to 10 m thick (Stow et al., 2013b; Hernández-Molina et al., 2014). Viana et al. (1998) suggested that these sandy contourites are independent of water depth, although most deposits have been described from intermediate water depth zones (300–2000 m) as extensive sandy sheets.

The HARs within contourites terraces in the Uruguayan margin could suggest the occurrence of sandy contourite deposits associated with terraces on top of plastered drifts. In other areas, sandy deposits are interpreted as sand overspill by shelf currents (e.g., storms, tides, trade winds, eddies, etc) (Viana et al., 1998; Kowsmann and de Carvalho, 2002); or pre-deposited sand layers exposed at the sea-floor to sweeping bottom currents (Faugères et al., 1999). In the Uruguayan continental margin the potential sandy deposits were probably transported offshore from the continental shelf due to the export of shelf waters along the BMC axis (Piola et al., 2008; Guerrero et al., 2014; Matano et al., 2014). Lateral migration of the BMC between glacial and interglacial stages, should have been a very effective mechanism of sediment transport for the shelf to deep-water setting within the observed latitude range.

The HARs and their association with sandy deposits and contourite terraces would represent new findings which can redirect petroleum companies to shift their targets for hydrocarbon exploration into deep-water in the near future. Sandy contourite deposits on terraces might represent potential hydrocarbon reservoirs and are therefore of potential interest to petroleum exploration efforts, especially if they are located at larger burial depths. The seismic amplitude and its associated varying sand content follow a simple concept: the stronger the currents, the coarser the sediments deposits; the thicker the deposit, the longer the current activity (Viana and Rebesco, 2007). Commonly, these deposits present good petrophysical characteristics, such as high values of porosity, permeability, and lateral and vertical transmissibility of fluids (Viana, 2008). As hydrocarbon exploration moves further into deeper water (>2000 m), large sedimentary deposits that have been affected/deposited by bottom currents are common in these setting including contourite terraces (Hernández-Molina et al., 2009; Preu et al.,

2013), giant sediment waves that run perpendicular to slope over these terraces (Duarte and Viana, 2007) and regional erosion surfaces (Faugères et al., 1999). Understanding how contour currents work along continental margins will assist hydrocarbon exploration with both reservoir presence and—due to the ability to rework in-place sands—reservoir quality (Viana, 2008; Mutti and Carminatti, 2012; Rebesco et al., 2014).

9. Conclusions

The regional morphosedimentary map of the Uruguayan continental margin demonstrates the occurrence of a large contourite depositional system as well as the interplay between down- and along-slope processes since the Eocene/Oligocene boundary. The contourite depositional system is composed of a spectacular array of identified sedimentary contourite depositional, erosional and mixed features characterizing a complex terraced slope. Bottom-current features occurrence on continental margins is common in many basins, but their occurrence along the Uruguayan margin demonstrate that: 1) they have large dimensions and good along-slope continuity; 2) contourite features are present event where other deep-water processes, as gravitational ones, are also dominant; 3) complex and different processes are identified related to certain water masses and their interfaces in a specific water depth, which have shaped the morphology of the continental margin and conditioned the stratigraphic stacking pattern.

The slope morphology is characterized by the occurrence of large contourite terraces along the margin, mainly on the middle slope due to action of the AAIW and on the base of the slope/upper rise due to the influence of the AABW mainly during glacial periods. Fluctuations of the Brazil/Malvinas Confluence (BMC) on geological scale are decoded with sedimentary and paleoceanographic implications on the location and intensity of the subtropical gyre in the entire South Atlantic. These fluctuations should have been related to variations in the wind pattern over the South Atlantic and further constrain general climatic and more regional/global ocean circulation models, but should be evaluated with more detail in future studies.

Contourite terraces contain high amplitude reflections (HARs), which could be related to sandy deposits, which might mark good reservoir deposits. In large drifts deposits muddy sediments dominate between submarine canyons, shaping the slope morphology. These drift deposits record important changes in the evolution of the margin being the Middle and Late Miocene the major stages in the sedimentary stacking pattern, with the establishment of the present circulation during the Pliocene and Quaternary and the development of the recent major contourite features. Some of these features, which are only observed due to the size and dense sampling of the seismic dataset, pose questions about our fundamental understanding of margin morphologies and bedform development in the deep marine environment.

Acknowledgments

The authors would like to thank ANCAP, Spectrum and BG Group for permission in using unpublished seismic datasets. We thank A. Viana (PETROBRAS, Brazil) and D. G. Borisov (Russian Academy of Sciences, Russia) for their helpful guidance in revising the manuscript prior to submission. Their input greatly improved the presentation of this research. The research was supported through the projects CTM 2012-39599-C03, and the Inter-American Institute for Global Change Research grants SGP2076 and CRN3070 (US National Science Foundation grant GEO-1128040). Finally, we also thank the reviewers Katrien Heirman (*Geological Survey of Denmark and Greenland*) and an anonymous reviewer for their very positive and helpful suggestions which helped us to improve the paper.

References

Benavides-Cáceres, V., 1999. Orogenic evolution of the Peruvian Andes: the Andean cycle. In: Skinner, B.J. (Ed.), Geology and mineral deposits of the central Andes. Society of Economic Geologists, Special Publication no. 7, pp. 61–107.

Blaich, O.A., Faleide, J.I., Tsikalas, F., Franke, D., León, E., 2009. Crustal-scale architecture and segmentation of the Argentine margin and its conjugate off South Africa. Geophys. J. Int. 178, 85–105.

Borisov, D.G., Murdmaa, I.O., Ivanova, E.V., Levchenko, O.V., Yutsis, V.V., Frantseva, T.N., 2013. Contourite systems in the region of the Southern São Paulo Plateau Escarpment, South Atlantic. Oceanology 53, 460–471.

Bozzano, G., Violante, R.A., Cerredo, M.E., 2011. Middle slope contourite deposits and associated sedimentary facies off NE Argentina. Geo-Mar. Lett. 31, 495–507.

Contreras, J., Zühlke, R., Bowman, S., Bechstädt, T., 2010. Seismic stratigraphy and subsidence analysis of the southern Brazilian margin (Campos, Santos and Pelotas basins). Mar. Pet. Geol. 27 (9), 1952–1980. http://dx.doi.org/10.1016/j.marpetgeo.2010.06.007.

Duarte, C.S.L., Viana, A.R., 2007. Santos Drift System: Stratigraphic organization and implications for late Cenozoic palaeocirculation in the Santos Basin. In: Viana, A.R., Rebesco, M. (Eds.), Economic and Palaeoceanographic Significance of Contourite Deposits. Geological Society, London, Special Publication 276, pp. 171–198.

Ewing, M., Lonardi, A.G., 1971. Sediment transport and distribution in the Argentine Basin. 5. Sedimentary structure of the Argentine margin, basin, and related provinces. Phys. Chem. Earth 8, 123–251.

Faugères, J.-C., Stow, D.A.V., 2008. Contourite Drifts: Nature, Evolution and Controls. In: Rebesco, M., Camerlenghi, A. (Eds.), Contourites. Elsevier, Amsterdam, Developments in Sedimentology 60, pp. 257–288.

Faugères, J.-C., Stow, D.A.V., Imbert, P., Viana, A.R., 1999. Seismic features diagnostic of contourite drifts. Mar. Geol. 162, 1–38.

Franco-Fraguas, P., Burone, L., Mahiques, M., Ortega, L., Urien, C., Muñoz, A., López, G., Marin, Y., Carranza, A., Lahuerta, N., de Mello, C., 2014. Hydrodynamic and geomorphological controls on surface sedimentation at the Subtropical Shelf Front–Brazil–Malvinas Confluence transition off Uruguay (Southwestern Atlantic Continental Margin). Mar. Geol. 349, 24–36. http://dx.doi.org/10.1016/j.margeo.2013.12.010.

Franke, D., Neben, S., Ladage, S., Schreckenberger, B., Hinz, K., 2007. Margin segmentation and volcano-tectonic architecture along the volcanic margin off Argentina/Uruguay, South Atlantic. Mar. Geol. 244, 46–67. http://dx.doi.org/10.1016/j.margeo.2007.06.009.

Georgi, D.T., 1981. Circulation of bottom waters in the southwestern South Atlantic. Deep Sea Res. Part A 28 (9), 959–979.

Goni, G.J., Bringas, F., DiNezio, P.N., 2011. Observed low frequency variability of the Brazil Current front. J. Geophys. Res. Oceans (1978–2012) 116 (C10).

Gordon, A.L., 1989. Brazil–Malvinas Confluence–1984. Deep Sea Res. Part A 36 (3), 359–384.

Gordon, A.L., Greengrove, C.L., 1986. Geostrophic circulation of the Brazil–Falkland Confluence. Deep Sea Res. Part A 33 (5), 573–585.

Gray, A. 2014, Seabed geomorphology and gas hydrate distribution, Offshore Uruguay MSc Thesis (Unpublished), University of Aberdeen. 82 pp.

Gruetzner, J., Uenzelmann-Neben, G., Franke, D., 2011. Variations in bottom water activity at the southern Argentine margin: indications from a seismic analysis of a continental slope terrace. Geo-Mar. Lett. 31, 405–417. http://dx.doi.org/10.1007/s00367-011-0252-0.

Guerrero, R.A., Piola, A.R., Fenco, H., Matano, R.P., Combes, V., Yi, C., James, C., Palma, E.D., Saraceno, M., Strub, P.T., 2014. The salinity signature of the cross-shelf exchanges in the southwestern Atlantic Ocean: satellite observations. J. Geophys. Res. Oceans 119, 7794–7810. http://dx.doi.org/10.1002/2014JC010113.

Habgood, E.L., Kenyon, N.H., Masson, D.G., Akhmetzhanov, A., Weaver, P.P.E., Gardner, J., Mulder, T., 2003. Deep-water sediment wave fields, bottom current sand channels and gravity flow channel-lobe systems: Gulf of Cadiz, NE Atlantic. Sedimentology 50, 483–510.

Hernández-Molina, F.J., Llave, E., Preu, B., Ercilla, G., Fontan, A., Bruno, M., Serra, N., Gomiz, J.J., Brackenridge, R.E., Sierro, F.J., Stow, D.A.V., García, M., Juan, C., Sandoval, N., Arnaiz, A., 2014. Contourite processes associated to the Mediterranean outflow water after its exit from the Gibraltar Strait: global and conceptual implications. Geology 42, 227–230.

Hernández-Molina, F.J., Paterlini, M., Violante, R., Marshall, P., de Isasi, M., Somoza, L., Rebesco, M., 2009. Contourite depositional system on the Argentine slope: an exceptional record of the influence of Antarctic water masses. Geology 37, 507–510. http://dx.doi.org/10.1130/G25578A.1.

Hernández-Molina, F.J., Serra, N., Stow, D.A.V., Llave, E., Ercilla, G., Van Rooij, D., 2011. Along-slope oceanographic processes and sedimentary products around the Iberian margin. Geo-Mar. Lett. 31, 315–341.

Henkel, S., Strasser, M., Schwenk, T., Hanebuth, T.J.J., Hüsener, J., Arnold, G.L., Winkelmann, D., Formolo, M., Tomasini, J., Krastel, S., Kasten, S., 2011. An interdisciplinary investigation of a recent submarine mass transport deposit at the continental margin off Uruguay. Geochem. Geophys. Geosyst. 12 (8), 1–19, Q08009. http://dx.doi.org/10.1029/2011GC003669.

Hinz, K., Neben, S., Schreckenberger, B., Roeser, H.A., Block, M., Souza, K.G.D., Meyer, H., 1999. The argentine continental margin north of 48°S: sedimentary successions, volcanic activity during breakup. Mar. Pet. Geol. 16, 1–25. http://dx.doi.org/10.1016/S0264-8172(98)00060-9.

Knutz, P.C., 2008. Paleoceanographic significance of contourite drifts. In: Rebesco, M., Camerlenghi, A. (Eds.), ContouritesDevelopments in Sedimentology vol. 60. Elsevier, Amsterdam, pp. 511–535.

Kowsmann, R.O., de Carvalho, M.-D., 2002. Erosional event causing gas-venting on the upper continental slope, Campos Basin, Brazil. Cont. Shelf Res. 22, 2345–2354.

Krastel, S., Wefer, G., Hanebuth, T., Antobreh, A., Freudenthal, T., Preu, B., Schwenk, T., Strasser, M., Violante, R., Winkelmann, D., Sampling Party, M.s.s., 2011. Sediment dynamics and geohazards off Uruguay and the de la Plata River region (northern

Argentina and Uruguay). Geo-Mar. Lett. 31, 271–283. http://dx.doi.org/10.1007/s00367-011-0232-4.
Lumpkin, R., Garzoli, S., 2011. Interannual to decadal changes in the western South Atlantic's surface circulation. J. Geophys. Res. Oceans (1978–2012) 116 (C1).
Maldonado, A., Bohoyo, F., Galindo-Zaldívar, J., Hernández-Molina, F.J., Lobo, F.J., Lodolo, E., Martos, Y.M., Pérez, L.F., Schreider, A.A., Somoza, L., 2014. A model of oceanic development by ridge jumping: opening of the Scotia Sea. Glob. Planet. Chang. 123, 152–173. http://dx.doi.org/10.1016/j.gloplacha.2014.06.010.
Masson, D.G., Wynn, R.B., Bett, B.J., 2004. Sedimentary environment of the Faeroe-Shetland Channel and Faeroe Bank channels, NE Atlantic, and the use of bedforms as indicators of bottom current velocity in the deep ocean. Sedimentology 51, 1–35.
Matano, R.P., Combes, V., Piola, A.R., Guerrero, R.A., Palma, E.D., Strub, P.T., James, C., Fenco, H., Chao, Y., Saraceno, M., 2014. The salinity signature of the cross-shelf exchanges in the southwestern Atlantic Ocean: numerical simulations. J. Geophys. Res. Oceans 119, 7949–7968. http://dx.doi.org/10.1002/2014JC010116.
Miller, K.G., Mountain, G.S., Wright, J.D., Browning, J.V., 2011. A 180-million-year record of sea level and ice volume variations from continental margin and deep-sea isotopic records. Oceanography 24 (2), 40–53. http://dx.doi.org/10.5670/oceanog.2011.26.
Morales, E., 2013. Evoluçao Tectônica e Estratigráfica das Bacias da Margem Continental do Uruguai. Tese de Doutoramento. UNESP, São Paulo (167 pp.).
Mutti, E., Barros, M., Possato, S., Rumenos, L., 1980. Deep-sea fan Turbidite Sediments Winnowed by Bottom-Currents in the Eocene of the Campos Basin, Brazilian Offshore. 1st IAS Eur. Meet. Abstr, p. 114.
Mutti, E., Carminatti, M., 2012. Deep-water sands in the Brazilian offshore basins: AAPG Search and Discovery article 30219. http://www.searchanddiscovery.com/documents/2012/30219mutti/ndx_mutti.pdf.
Nelson, C.H., Baraza, J., Maldonado, A., 1993. Mediterranean undercurrent sandy contourites, Gulf of Cadiz, Spain. Sediment. Geol. 82, 103–131.
Olson, D.B., Podestá, G.P., Evans, R.H., Brown, O.B., 1988. Temporal variations in the separation of Brazil and Malvinas currents. Deep Sea Res. Part A 35 (12), 1971–1990.
Piola, A.R., Franco, B.C., Palma, E.D., Saraceno, M., 2013. Multiple jets in the Malvinas Current. J. Geophys. Res. Oceans 118, 2107–2117. http://dx.doi.org/10.1002/jgrc.20170.
Piola, A.R., Gordon, A.L., 1989. Intermediate waters in the southwest South Atlantic. Deep-Sea Res. 36 (1), 16.
Piola, A.R., Matano, R.P., 2001. Brazil and Falklands (Malvinas) currents. Academic Press, London.
Piola, A.R., Möller Jr., O.O., Guerrero, R.A., Campos, E.J.D., 2008. Variability of the subtropical shelf front off eastern South America: winter 2003 and summer 2004. Cont. Shelf Res. 28 (13), 1639–1648. http://dx.doi.org/10.1016/j.csr.2008.03.013.
Preu, B., Hernández-Molina, F.J., Violante, R., Piola, A.R., Paterlini, C.M., Schwenk, T., Voigt, I., Krastel, S., Spiess, V., 2013. Morphosedimentary and hydrographic features of the northern Argentine margin: The interplay between erosive, depositional and gravitational processes and its conceptual implications. Deep-Sea Res. I Oceanogr. Res. Pap. 75, 157–174. http://dx.doi.org/10.1016/j.dsr.2012.12.013.
Preu, B., Schwenk, T., Hernández-Molina, F.J., Violante, R., Paterlini, M., Krastel, S., Tomasini, J., Spieß, V., 2012. Sedimentary growth pattern on the northern Argentine slope: The impact of North Atlantic Deep Water on southern hemisphere slope architecture. Mar. Geol. 329–331, 113–125. http://dx.doi.org/10.1016/j.margeo.2012.09.009.
Rebesco, M., Camerlenghi, A. (Eds.), 2008. Developments in Sedimentology 60. Elsevier, Amsterdam.
Rebesco, M., Hernández, M.J., van Rooij, D., Wåhlin, A., 2014. Contourites and associated sediments controlled by deep-water circulation processes: state-of-the-art and future considerations. Mar. Geol. 352, 111–154. http://dx.doi.org/10.1016/j.margeo.2014.03.011.
Rossello, E.A., López-Gamundi, O., Veroslavsky, G., 2009. Influencias de la tectónica andina sobre la plataforma continental Atlántica (Uruguay-Argentina)?: Controles sobre su potencial exploratorio. X Simposio Bolivariano Exploración Petrolera en Cuencas Subandinas, Cartagena, julio de 2009.
Saraceno, M., Provost, C., Piola, A.R., Gagliardini, A., Bava, J., 2004. The Brazil Malvinas frontal system as seen from nine years of AVHRR data. J. Geophys. Res. 109 (C5), C05027. http://dx.doi.org/10.1029/2003JC002127.
Schlitzer, R., 2013. Ocean Data View. http://odv.awi.de.
Shanmugam, G., 2006. Deep-Water Processes and Facies Models: Implications for Sandstone Petroleum Reservoirs: 5. Handbook of Petroleum Exploration and Production. Elsevier Science (496 pp.).
Shanmugam, G., 2012. New perspectives on deep-water sandstones: origin, recognition, initiation, and reservoir quality. Handbook of Petroleum Exploration and Production vol. 9. Elsevier, Amsterdam, p. 524.
Shanmugam, G., Spalding, T.D., Rofheart, D.H., 1993. Process sedimentology and reservoir quality of deep-marine bottom-current reworked sands (sandy contourites): an example from the gulf of Mexico. Am. Assoc. Pet. Geol. Bull. 77, 1241–1259.
Soto, M., Morales, E., Veroslavky, G., De Santa Ana, H., Ucha, N., Rodríguez, P., 2011. The continental margin of Uruguay: crustal architecture and segmentation. Mar. Pet. Geol. 28, 1676–1689. http://dx.doi.org/10.1016/j.marpetgeo.2011.07.001.
Stica, J.M., Zalán, P.V., Ferrari, A.L., 2014. The evolution of rifting on the volcanic margin of the Pelotas Basin and the contextualization of the Paraná-Etendeka LIP in the separation of Gondwana in the South Atlantic. Mar. Pet. Geol. 50, 1–21.
Stoakes, F.A., Campbell, C.V., Cass, R., Ucha, N., 1991. Seismic stratigraphic analysis of the Punta del Este Basin, offshore Uruguay, South America. Bull. Am. Assoc. Pet. Geol. 75 (2), 219–240.
Stoker, M.S., Akhurst, M.C., Howe, J.A., Stow, D.A.V., 1998. Sediment drifts and contourites on the continental margin off northwest Britain. Sediment. Geol. 115, 33–51.
Stow, D.A.V., Hernández-Molina, F.J., Alvarez Zarikian, C.A., the Expedition 339 Scientists, 2013b. Proceedings IODP, 339. Integrated Ocean Drilling Program Management International, Tokyo. http://dx.doi.org/10.2204/iodp.proc.339.2013.
Stow, D.A.V., Hernández-Molina, F.J., Llave, E., Bruno, M., García, M., Díaz del Río, V., Somoza, L., Brackenridge, R.E., 2013a. The Cadiz Contourite Channel: sandy contourites, bedforms and dynamic current interaction. Mar. Geol. 343, 99–114.
Stramma, L., England, M., 1999. On the water masses and mean circulation of the South Atlantic Ocean. J. Geophys. Res. 104 (C9), 20,863–20,883. http://dx.doi.org/10.1029/1999JC900139.
Sykes, T.J.S., Ramsay, T.S., Kidd, R.B., 1998. Southern hemisphere Miocene bottom-water circulation: a palaeobathymetric analysis. In: Cramp, A.A., MacLeod, C.J., Lee, S.V., Jones, E.J.W. (Eds.), Geological evolution of ocean basin: results from the ocean drilling program. Geological Society of London 131, pp. 43–54.
Thompson, P., Badalini, G., Wrigley, S., Hendy, J., Walker, R., Argent, J., Soto, M., de Santa Ana, H., Gristo, P., Hernández-Molina, F.J., 2015. Travelling without moving: ever-changing seabed morphology and the influence of contour currents, from cretaceous to present-day, within the Pelotas Basin, Offshore Uruguay. IAS 31st Meeting of Sedimentology, Kraków, 22nd-25th June 2015 (Abstract volume).
Tomasini, J., de Santa Ana, H., Conti, B., Ferro, S., Gristo, P., Marmisolle, J., Morales, E., Rodríguez, P., Soto, M., Veroslavsky, G., 2011. Assessment of marine gas hydrates and associated free gas distribution offshore Uruguay. J. Geophys. Res., 326259 http://dx.doi.org/10.1155/2011/326250 (7 pp.).
Viana, A.R., 2001. Seismic expression of shallow- to deep-water contourites along the south-eastern Brazilian margin. Mar. Geophys. Res. 22, 509–521.
Viana, A.R., 2008. Economic Relevance of Contourites. In: Rebesco, M., Camerlenghi, A. (Eds.), ContouritesDevelopments in Sedimentology 60. Elsevier, Amsterdam, pp. 493–510.
Viana, A.R., Rebesco, M. (Eds.), 2007. Economic and Palaeoceanographic Significance of Contourite DepositsGeological Society 276. Special Publication, London.
Viana, A.R., Almeida Jr., W., Almeida, C.F.W., 2002a. Upper Slope Sands–the Late Quaternary Shallow-Water Sandy Contourites of Campos Basin SW Atlantic Margin. In: Stow, D.A.V., Pudsey, C.J., Howe, J.A., Faugères, J.C., Viana, A.R. (Eds.), Deep-Water Contourite Systems: Modern Drifts and Ancient Series, Seismic and Sedimentary Characteristics. Geological Society, London, Memoirs 22, pp. 261–270.
Viana, A.R., Faugères, J.C., 1998. Upper Slope Sand Deposits: The Example of Campos Basin, a Latest Pleistocene/Holocene Record of the Interaction Between Along and Across Slope Currents. In: Stoker, M.S., Evans, D., Cramp, A. (Eds.), Geological Processes on Continental Margins–Sedimentation, Mass-Wasting and Stability. Geological Society, London, Special Publication 129, pp. 287–316.
Viana, A.R., Faugères, J.C., Stow, D.A.V., 1998. Bottom-current controlled sand deposits: a review from modern shallow to deep water environments. Sediment. Geol. 115, 53–80.
Viana, A.R., Hercos, C.M., Almeida Jr., W., Magalhães, J.L.C., Andrade, S.B., 2002b. Evidence of Bottom Current Influence on the Neogene to Quaternary Sedimentation Along the Northern Campos Slope, SW Atlantic Margin. In: Stow, D.A.V., Pudsey, C.J., Howe, J.A., Faugères, J.C., Viana, A.R. (Eds.), Deep-Water Contourite Systems: Modern Drifts and Ancient Series, Seismic and Sedimentary Characteristics. Geological Society, London, Memoirs 22, pp. 249–259.
Violante, R.A., Paterlini, C.M., Costa, I.P., Hernández-Molina, F.J., Segovia, L.M., Cavallotto, J.L., Marcolini, S., Bozzano, G., Laprida, C., García Chapori, N., Bickert, T., Spieß, V., 2010. Sismoestratigrafia y evolución geomorfológica del talud continental adyacente al Litoral del Este bonaerense, Argentina. Latin American Journal of Sedimentology and Basin Analysis vol. 7, pp. 33–62.
Vivier, F., Provost, C., 1999. Direct velocity measurements in the Malvinas Current. J. Geophys. Res. Oceans (1978–2012) 104 (C9), 21083–21103.
Yrigoyen, M.R., 1979. Cordillera principal. Actas del II Simposio de Geología Regional Argentina vol. 1. Academia Nacional de Ciencias, pp. 651–694 (Córdoba).
Zachos, J., Pagani, H., Sloan, L., Thomas, E., Billups, K., 2001. Trends, rhythms, and aberrations in global climate 65 Ma to present. Science 292, 686–693.

Further reading

Viana, A.R., Faugères, J.C., Kowsmann, R.O., Lima, J.A.M., Caddah, L., Rizzo, J.G., 1998. Hydrology, morphology and sedimentology of the Campos continental margin, offshore Brazil. Sediment. Geol. 115, 133–157.